

## Reply to Reviewer 1

Reviewer: Understanding the compound dry and hot events is very important to human being society and environments. This study proposes a new compound drought and heat index on daily scale, SCDHI, based on SAPEI and STI. This index is useful to quantify sub-monthly characteristics of compound dry and hot events. The topic is very interesting and suitable for HESS. I recommend the manuscript for acceptance with a minor revision. The detailed comments are provided below:

*Author's reply:* We highly appreciate the constructive comments and suggestions.

Reviewer (1): This study focuses the non-arid areas in China. Is SCDHI suitable for the arid areas?

*Author's Reply (1):* Thank you for your comment. In this study, we did not assess the application of SCDHI in arid areas in China, because of three reasons: (1) replenishment of water resources in the Chinese arid region is mainly from melted glacial or perennial frozen soil, and not from precipitation. The statistical drought indices are usually limited its role in revealing drought in such complex situation. (2) meteorological observations in Chinese arid regions are too scarce to conduct robust analysis (Wu et al., 2007; Xu et al., 2015). (3) From a practical perspective, calculating climate extreme indices across arid region with large-scale desert regions is less meaningless (Tomas-Burguera et al., 2020). Thus, we did not evaluate the application of SCDHI in arid region. In further study, we will try to develop the compound dry-hot index adopted arid regions.

We have added explanation in Lines 154-161.

### Reference:

- Tomas-Burguera, M., Vicente-Serrano, S. M., Peña-Angulo, D., Domínguez-Castro, F., Noguera, I., & El Kenawy, A. Global characterization of the varying responses of the Standardized Evapotranspiration Index (SPEI) to atmospheric evaporative demand (AED). *Journal of Geophysical Research: Atmospheres*, e2020JD033017.
- Xu, K., Yang, D., Yang, H., Li, Z., Qin, Y., & Shen, Y. (2015). Spatio-temporal variation of drought in China during 1961–2012: A climatic perspective. *Journal of Hydrology*, 526, 253-264.
- Wu, H., Svoboda, M. D., Hayes, M. J., Wilhite, D. A., & Wen, F. (2007). Appropriate application

of the standardized precipitation index in arid locations and dry seasons. *International Journal of Climatology: A Journal of the Royal Meteorological Society*, 27(1), 65-79.

Reviewer (2): There was a similar index for characterizing CDHEs (Hao et al., 2020). I suggest the authors to discuss the difference between this study and the study of Hao et al. (2020), and highlight the novelty of this study in the Introduction section. Hao, Z., Hao, F., Singh, V. P., Ouyang, W., Zhang, X., & Zhang, S. (2020). A joint extreme index for compound droughts and hot extremes. *Theoretical and Applied Climatology*, 1-8.

Author's Reply (2): Thank you for your recommendation. The study of Hao et al. (2020) provides a good background for our study and partially inspired the idea to develop SCDHI.

We have added discussion in Lines 73-83.

Reviewer (3): Why is the growing season selected to identify CDHEs in Section 3.3? Please explain a little bit more on it.

Author's Reply (3): Thank you for your comment and suggestion. The compound dry-hot events were examined during the approximate growing season (April-September) because this is the time where they can cause major impacts. Due to the strong seasonal cycle in temperature and precipitation and focusing on relative exceedance thresholds, mixing seasons could result in results that are difficult to interpret.

We have added explanation in Lines 526-527.

Reviewer (4): Abstract: the regional difference exists in the future change of the CDHE characteristics. The authors may want to add this in the abstract.

Author's Reply (4): Thank you for your suggestion. Indeed, there are difference between region for future change of the CDHE characteristics. Specifically, under RCP 8.5 scenario, CDHE in the central to west parts of China is expected to markedly increase by more than five times; duration in mid-west China potentially increases by approximately 1.5 times; severity over mid-west China is expected to more than triple under RCP 8.5.

We have added these contents in Abstract. Please see Lines 34-36.

Reviewer (5): P143: how reliable is interpolated data based on the kriging method? Did the author evaluate the interpolated 0.25-degree data?

Author's Reply (5): Thank you for your questions. A reliable interpolation method is important to provide fundamental data for research. To generate reliable gridded data in China, previous studies have compared different interpolation methods (e.g., ordinary nearest neighbor, local polynomial, radial basis function, inverse distance weighting, and ordinary kriging), and they found that the ordinary kriging method shows the best performance and yields higher interpolation accuracy than the other methods (Chen et al., 2010; Lin et al., 2002).

Datasets based on the kriging method have also been used extensively for drought analyses (Liu et al., 2016; Wu et al., 2013; Shen et al., 2019). Based on these previous research findings, the kriging method was thus used in this study, and we did not evaluate the kriging method but rely on previous findings.

We have added explanation in Lines 151-154.

#### Reference:

- Chen, D., Ou, T., Gong, L., Xu, C. Y., Li, W., Ho, C. H., & Qian, W. (2010). Spatial interpolation of daily precipitation in China: 1951–2005. *Advances in Atmospheric Sciences*, 27(6), 1221-1232.
- Lin, Z. H., Mo, X. G., Li, H. X., & Li, H. B. (2002). Comparison of three spatial interpolation methods for climate variables in China. *Acta Geographica Sinica*, 57(1), 47-56.
- Liu, Z., Wang, Y., Shao, M., Jia, X., & Li, X. (2016). Spatiotemporal analysis of multiscalar drought characteristics across the Loess Plateau of China. *Journal of Hydrology*, 534, 281-299.
- Shen, Z., Zhang, Q., Singh, V. P., Sun, P., Song, C., & Yu, H. (2019). Agricultural drought monitoring across Inner Mongolia, China: Model development, spatiotemporal patterns and impacts. *Journal of Hydrology*, 571, 793-804.
- Wu, J., Zhou, L., Liu, M., Zhang, J., Leng, S., & Diao, C. (2013). Establishing and assessing the Integrated Surface Drought Index (ISDI) for agricultural drought monitoring in mid-eastern China. *International Journal of Applied Earth Observation and Geoinformation*, 23, 397-410.

Reviewer (6): P152: what is the standard number of GB/T 20481-2017? It would be clearer if the authors add some more information on it.

Author's reply (6): Thank you for your question and suggestion. The PDSI is a semi physical drought index based on the land surface water balance. The parameters of the standardized procedure of the conventional PDSI, including the climatic characteristic

and duration factors, are empirically derived using the meteorological data of the central USA with its semi-arid climate. Therefore, the portability and spatial comparability of the conventional PDSI are relatively poor in other regions of the world. To develop a PDSI suited for China, the PDSI calculation procedure was revised based on long-term meteorological data of several in-situ stations distributed around China that represent the climate characteristic of mainland China. A China national standard of classification of meteorological drought with standard number of GB/T 20481–2017 provides the corrected calculation procedure of the PDSI specific for China:

$$Z_i = K_m d_i \quad (1)$$

$$K_m = \left( \frac{16.84}{\sum_{j=1}^{12} \overline{D}_j K'_m} \right) K'_m \quad (2)$$

$$K'_m = 1.6 \log_{10} \left[ \left( \frac{\overline{PE}_m + \overline{R}_m + \overline{RO}_m}{\overline{P}_m + \overline{L}_m} + 2.8 \right) / \overline{D}_m \right] + 0.4 \quad (3)$$

$$X_i = 0.755 X_{i-1} + Z_i / 1.63 \quad (4)$$

We have added the calculation procedure of PDSI of the GB/T 20481–2017 in supplementary material.

Reviewer (7): P155: soil moisture data in different depths is available in the GLDAS product. Why did the authors choose the root zone soil moisture to evaluate the drought indices? How about soil moisture in the surface layer and in total column?

Author's reply (7): Thank you for your questions and comments. Some soil moisture datasets in the GLDAS product provides different depths. For instance, the NOAH model of GLDAS has total of 4 layers thickness: 0-10, 10-40, 40-100, and 100-200 cm, while NOAH only has monthly temporal resolution. The CLSM product used in this study does not have explicit vertical levels, instead soil moisture is represented in Surface (0-2cm), and Root Zone (0-100cm). Root zone soil moisture is chosen over the surface soil moisture on account of its appositeness to characterize drought and low noise relative to surface soil moisture (Hunt et al., 2009; Osman et al., 2020). For drought monitoring, this product has the advantage of offering spatially and temporally complete root zone soil moisture estimates on a grid. Furthermore, standard drought indices based on a time scale of three months (or higher) seem to more representative

of drought behavior in deeper soil layers (Fig. 6 in Nicolai-Shaw et al., 2017).

We have added illustration in Lines 175-179.

Reference:

Hunt, E. D., Hubbard, K. G., Wilhite, D. A., Arkebauer, T. J., & Dutcher, A. L. (2009). The development and evaluation of a soil moisture index. *International Journal of Climatology*, 29(5), 747-759.

Nicolai-Shaw, N., J. Zscheischler, M. Hirschi, L. Gudmundsson, and S. I. Seneviratne (2017). A drought event composite analysis using satellite remote-sensing based soil moisture. *Remote Sensing of Environment* 203, 216-225.

Osman, M., Zaitchik, B. F., Badr, H. S., Christian, J. I., Tadesse, T., Otkin, J. A., & Anderson, M. C. (2020). Flash drought onset over the Contiguous United States: Sensitivity of inventories and trends to quantitative definitions. *Hydrology and Earth System Sciences Discussions*, 1-21.

Reviewer (8): P163: the resolutions of eight climate models are different. Are the results from these models resampled to the same resolution?

Author's reply (8): Thank you for your question. We are sorry that we did not provide a clear description of how the data was processed.

Earth system models (ESMs) provide useful information of future climate projections through global-scale simulations. However, the coarse resolution of ESMs restricts their usefulness for many sub-region-scale applications, requiring downscaling of climate model output (Chen et al., 2019; Fenta and Disse, 2018). In this study, the bias-corrected climate imprint method (Werner and Cannon, 2016), a statistical downscaling method based on the delta approach, was applied to downscale the climate model output to a spatial resolution of 0.25°.

We have added illustration in Lines 201-203.

Reference:

Werner, A. T., & Cannon, A. J. (2016). Hydrologic extremes—an intercomparison of multiple gridded statistical downscaling methods. *Hydrology and Earth System Sciences*, 20(4), 1483.

Reviewer (9): P164: five is missing after phase.

Author's reply (9): Thank you for your comment. We have done.

Reviewer (10): P448: what does the national weather reports look like? I did not

see the information on the two CDHEs from the national weather reports.

Author's reply (10): Thank you for your question. The national weather report is a public service product provided by China Meteorological Administration (<http://www.weather.com.cn/>). Specifically, the CDHE in Sichuan-Chongqing region during summer of 2006 is reported in <http://www.weather.com.cn/zt/kpzt>, while the other event during July to September of 2009 was recorded in Yearbook of Meteorological Disasters in China 2010.

We have added illustration Lines 518-519.

Reviewer (11): Figs. 3 and 5: is soil moisture is represented by the standardized anomaly? If yes, please briefly describe this. And what is the solid black line all the way from the beginning time down to the ending time?

Author's reply (11): Thank you for your questions and suggestions. The soil moisture in Figure 3 and 5 represents the standardized anomaly. To avoid the effect of seasonality, the soil moisture was fitted by Gamma probability distribution, and then was standardized by normal quantile transformation. The value of solid black line is at -0.5, indicating the distinction between drought and non-drought according to our definition.

We have added illustrations in Lines 183-185 and Figure 3 and 5:

Reviewer (12): Figs. 4, 6, and 10: please add the longitude and latitude on the figures.

Author's reply (12): Thank you for your comment. We have added the longitude and latitude on the figures. Please see Figure 4, 6, 8, and 9.

Reviewer (13): Fig. 8: I cannot see the difference among three panels in the last line. Is it because an inappropriate colorbar is used?

Author's reply (13): Thank you for your comment. We have revised the figure. Please see Figure 7.

Reviewer (14): Figure 11d): the numbers 1.8 and 2 in the colorbar are placed wrongly. They should be exchanged.

Author's reply (14): Thank you for your comment. We are sorry for the mistake and

will check throughout the manuscript to avoid similar mistakes. We have revise the figure. Please see Figure 10.

Reviewer (15): Figs. 12 and 13: is the historical period used here 1961-2005 or 1951-2018? The authors mentioned that they obtained the model outputs for the 1961-2005 period in Section 2.1. However, the 1961-2005 period does not show up in the results. And is the historical data from the CMIP5 climate models or from the interpolated observations? If the observational data is used as the reference, how the authors resolve the resolution difference between the observational data and the model results?

Author's reply (15): Thank you for your comments and question. In Figure 12 and 13 of the first-round manuscript, the historical periods are from 1961 to 2018, and the observational datasets were used. To match the spatial scale, the bias-corrected climate imprint method, was applied to bias correct and downscale the model output to same resolution in this study (see Author's reply (8)).

Reference:

Werner, A. T., & Cannon, A. J. (2016). Hydrologic extremes—an intercomparison of multiple gridded statistical downscaling methods. *Hydrology and Earth System Sciences*, 20(4), 1483.

Reviewer (16): Please check through the manuscript and correct all the grammar mistakes.

Author's reply (16): Thank you. We have checked the revision thoroughly for grammar mistakes.

## Reply to Reviewer 2

Reviewer: Interesting objective, interesting method, but hard to read.

Author's reply: Thank you for your comments and suggestions.

Reviewer (1): (a) The paper discusses a standardized index for assessing compound dry and hot conditions. Overall, I find the paper not in a really good shape, and I have to admit that I found it really hard to read due to the excessive amount of acronyms. The paper is so technical that for a reader who does know something about the topic, it is still very hard to follow. (b) For me it did not become entirely clear what are now the new insights that can be learned by creating this new index that were not known before. (c) I also think that the authors should make a new selection of figures and reduce the paper to the essentials, because with the figures in the text and the supplementary material there are so many panels showing China that it becomes overwhelming to the reader. I put some comments below that could help in improving the paper.

Author's reply: Thank you for your comments and suggestions.

(a) We are sorry for the excessive number of acronyms. We have strongly reduced the utilization of the abbreviations in revised manuscript.

(b) Please allow us to clarify the new insights of this index:

Much effort has been made to study the compound dry-hot event in recent years. Utilizing thresholds to define the concurrent events, the frequency of compound events has received much attention (Wu et al., 2019; Zhang et al., 2019). However, this approach fails to measure compound event characteristics (e.g., duration, severity, and intensity), and is inconvenient for comparing compound event characteristics through different climates (Wu et al., 2020). Several indices were thus proposed for analyzing the characteristics of the compound events, such as standardized compound event indicator and standardized compound dry-hot index. These indices provide useful tools to understanding compound dry-hot event characteristics. However, they are subject to some shortcomings including the fixed monthly scale and the disregard of evapotranspiration, which may limit their use in monitoring the detailed evolution of compound dry and hot events.

In addition, severe concurrent drought and heat can suddenly strike a region within



short duration when extreme weather anomalies persist over the same region (Röthlisberger and Martius, 2019; Wang et al., 2016). Concurrent short-term drought and heatwaves can pose great socio-economic risks (Zhang et al., 2019). There is thus a need to have readily available indices capable of monitoring sub-monthly compound dry-hot conditions. A suite of indices have been proposed for the assessments of droughts and heatwaves separately, yet there is no index available for incorporating the joint variability of dry and hot conditions at sub-monthly scale.

The proposed SCDHI index provides a new tool to monitor and quantify the characteristics of compound dry-hot events at multiple time scale (e.g., daily, weekly and monthly) to provide detailed information on their initiation, development, termination, and trends.

We have rewritten the motivation and benefits of this new index in Lines 125-140.

(c) We agree that the figures in the first-round manuscript need to be reduced. Specifically, as the results on 3, 6, 9, 12-month scale SAPEI/SCDHI in Figure 2, 4, 6, 8, 9, 10 are generally similar, we have only shown results on 3-month scale SAPEI/SCDHI, and removed the similar results on other time scales in these Figures. In addition, we have removed the Figure 7 and 13 in revised manuscript.

The supplementary materials mainly involve the metrics for selecting copula, and assessment of SAPEI/SCDHI ability to monitor monthly drought/compound dry-hot conditions using real-world typical events. These analyses are necessary but not essential, so placing them in the supplementary material without adding manuscript space. We have reduced the text content related to supplementary materials, and subfigures in supplementary materials, but kept essential figure and content to ensure the integrity of paper structure.

#### Reference:

- Röthlisberger, M. and Martius, O.: Quantifying the Local Effect of Northern Hemisphere Atmospheric Blocks on the Persistence of Summer Hot and Dry Spells, *Geophys. Res. Lett.*, doi:10.1029/2019GL083745, 2019.
- Wang, L., Yuan, X., Xie, Z., Wu, P. and Li, Y.: Increasing flash droughts over China during the recent global warming hiatus, *Sci. Rep.*, doi:10.1038/srep30571, 2016.
- Wu, X., Hao, Z., Hao, F. and Zhang, X.: Variations of compound precipitation and temperature extremes in China during 1961–2014, *Sci. Total Environ.*, 663, 731–737,

doi:10.1016/j.scitotenv.2019.01.366, 2019.

Wu, X., Hao, Z., Zhang, X., Li, C. and Hao, F.: Evaluation of severity changes of compound dry and hot events in China based on a multivariate multi-index approach, *J. Hydrol.*, 583, 124580, doi:10.1016/j.jhydrol.2020.124580, 2020.

Zhang, Y., You, Q., Mao, G., Chen, C. and Ye, Z.: Short-term concurrent drought and heatwave frequency with 1.5 and 2.0 °C global warming in humid subtropical basins: a case study in the Gan River Basin, China, *Clim. Dyn.*, 52(7–8), 4621–4641, doi:10.1007/s00382-018-4398-6, 2019.

Reviewer (2): It could be good to mention already in the title that this study only concerns China. The paper does not deliver a universal index for compound dry and hot conditions, but one that is only developed for application in China.

Author's reply (2): Thank you for your comments and suggestions. Because developing a sub-monthly index requires datasets with high temporal resolution (e.g., daily precipitation, maximum air temperature, mean air temperature, minimum air temperature, relative humidity, wind speed, and sunshine duration), it is difficult to collect all these daily datasets on a global scale. While the index is computed for China base on readily available datasets, the methodology is universal.

China has vast territory and complex and diverse climates, and during the past decades, it suffers from frequent and severe compound dry-hot events (Wu et al., 2019). Overall, it serves as an excellent setting to study compound dry-hot events.

We have changed the title into: “A standardized index for assessing sub-monthly compound dry and hot conditions: application in China”

#### Reference:

Wu, X., Hao, Z., Zhang, X., Li, C., & Hao, F. (2019). Evaluation of severity changes of compound dry and hot events in China based on a multivariate multi-index approach. *Journal of Hydrology*, 583, 124580.

Reviewer (3): As a reviewer, it did not become completely clear to me what the exact problem is of combined dry and hot conditions. There are many examples, but their explanation does not really get to the core: why do we need an indicator for dry and hot? Please improve this in the revision.

Author's reply (3): Thank you. Different combinations of dry and hot conditions

lead to different types of impacts including crop failure vegetation impacts or wild fires. Thereby it matters hot and dry it really is. Slightly hotter conditions may exacerbate impacts from dry conditions (Ribeiro et al., 2020). Furthermore, the correlation between hot and dry conditions render a naive combination of univariate indicators of hot and dry events unsuitable for estimating combined impacts. A combined dry-hot indicator implicitly accounts for the dependence between hot and dry conditions and provides a univariate metric to measure the intensity of combined stress due to heat and drought. For crops it has been shown that such a bivariate indicator can explain crop yield better than typically used linear regression models (Zscheischler et al., 2017).

The author's reply (1) has provided further motivation for such an index. We have reduced the number of given examples, and written the introduction. Please see Lines 44-140.

#### Reference:

- Ribeiro, A. F. S., Russo, A., Gouveia, C. M., Páscoa, P., and Zscheischler, J.: Risk of crop failure due to compound dry and hot extremes estimated with nested copulas, *Biogeosciences Discuss.*, in review, 2020.
- Zscheischler, J., Orth, R., and Seneviratne, S. I.: Bivariate return periods of temperature and precipitation explain a large fraction of European crop yields, *Biogeosciences*, 14, 3309–3320, 2017.

Reviewer (4): I find the methods a little ill-described. There are many references back to previous papers, but please list the equations of the equations that you take from these papers, because now the reader has to look up essential information in previous papers. Also, please be exact what the source of the input data is that is needed to compute all the variables that you need.

Author's reply (4): Thank you for your comments and suggestions. We are sorry for the unclear description on methods. In this study, only the SAPEI involve the previous papers, and the manuscript have already shown the equations that were used to calculate this index, i.e., equation (1).

The SCDHI calculation relies on STI and SAPEI. STI is calculated from maximum temperature, while SAPEI is calculated from precipitation and potential evapotranspiration. The Penman-Monteith method is used to calculate the potential evapotranspiration, requiring maximum air temperature, mean air temperature,

minimum air temperature, relatively humidity, wind speed, and sunshine duration.

We have added illustration in Lines 214-216.

Reviewer (5): Line 203: how does one use a probability distribution to create daily time series, and against what is it fitted? I do not understand the procedure.

Author's reply (5): Thank you for your question. The probability is not used to create daily time series, but applied to fit a time series.

Please allow us to show a case for SAPEI calculation:

Taking the calculation of SAPEI on May 1 of each year (1961-2018) as an example, with respect to 3-month scale SAPEI, the total water surplus or deficit in three months before May 1 of each year is calculated to represent the dry and wet condition on May 1, and thus, there are 58 values representing the dry and wet conditions on May 1 of each year from 1961 to 2018. The water surplus or deficit was calculated through the difference between precipitation and potential evapotranspiration. For calculating a standardized index, a probability distribution was used to fit the daily time series (58 values), which was then transformed into a standard normal distribution (resulting in the SAPEI) using the classical approach of Barton et al. (1965).

We have added a case of SAPEI calculation in supplementary materials.

Reference:

Barton, D. E., Abramovitz, M. and Stegun, I. A.: Handbook of Mathematical Functions with Formulas, Graphs and Mathematical Tables., J. R. Stat. Soc. Ser. A, doi:10.2307/2343473, 1965.

Reviewer (6): Line 219: what is copula theory?

Author's reply (6): Thank you for your question.

Developed by Sklar (1959), copulas are functions that link univariate distribution functions to form multivariate distribution functions. The merit of using copulas to construct multivariate distributions is that copulas can separate the dependence effects from the marginal distribution effects. Construction of multivariate distribution is thus reduced to studying the relations among the correlated random variables if marginal distributions are given.

Considering a situation with two random variables, Sklar's Theorem states that if  $F_{X,Y}(x, y)$  is a two-dimensional distribution function with marginal distributions  $F_X(x)$

and  $F_Y(y)$ , then there exists a copula  $C$  such that:

$$F_{X,Y}(x, y) = C(F_X(x), F_Y(y)) \quad (1)$$

Conversely, for any univariate distributions  $F_X(x)$  and  $F_Y(y)$  and any copula  $C$ , the function  $F_{X,Y}(x, y)$  defined above is a two-dimensional distribution function with marginal distributions  $F_X(x)$  and  $F_Y(y)$ . Furthermore, if  $F_X(x)$  and  $F_Y(y)$  are continuous, then  $C$  is unique.

Under the assumption that the marginal distributions are continuous with probability density functions  $f_X(x)$  and  $f_Y(y)$ , the joint probability density function then becomes

$$f_{X,Y}(x, y) = c(F_X(x), F_Y(y))f_X(x)f_Y(y) \quad (2)$$

Where  $c$  is the density function of  $C$ .

Books of Nelsen (2006) introduce a copula theory in detail.

We have added a brief introduction of copula theory in supplementary materials.

#### Reference:

Sklar, K.: Fonctions de repartition a n Dimensions et Leura Marges, Publ. Inst. Stat. Univ. Paris, 8, 229–231, 1959

Reviewer (7): Lines 226-250: This could use some explanatory figures. It is nearly impossible to understand for a reader that is not familiar with the specialized methods that are used here.

Author's reply (7): Thank you for your comment and suggestion. Figure S4 in supplementary material have already illustrated the SCDHI development.

Reviewer (8): Line 265: I think that there are more appropriate and far older references for the definition of the POD and FAR.

Author's reply (8): Thank you for your suggestion. We have added the reference:

“Winston, H.A., Ruthi, L.J.: Evaluation of RADAP II severe-storm-detection algorithms. Bull. Am. Meteorol. Soc., 67(2), 145-150, 1986.”

Reviewer (9): Section 3.1: What is the added value from SAPEI compared to much simpler metrics as soil moisture, or if that is not available P-E, or an simple estimation of evapotranspiration?

Author's reply (9): That is a good question and is basically related to the lack of

availability of soil moisture data.

Soil moisture would be the most appropriate variable for agriculture drought monitoring and analyses (Mishra and Singh, 2010). However, there are few long-term and large-scale observational soil moisture datasets due to insufficient observation stations around the world, especially for developing regions, which limits its wide use in drought monitoring and analyses. Thus, using observational hydrometeorological datasets, the complex physical process models, such as the Community Land Model, are widely used to simulate the soil moisture. However, running such models requires highly trained personnel not usually available at local agencies. In addition, when the model is used locally, it generally needs to be calibrated and verified by observational soil moisture and other hydrometeorological datasets. This certainly limits the wide use of soil moisture as a drought indicator.

An evapotranspiration-based drought index provides a useful tool for drought monitoring and analyses. However, in many regions and operational settings, evapotranspiration is derived from potential evapotranspiration (PET) through parameterizations of soil-water and plant-water availabilities that are of questionable value on operational space and time scales: in such cases PET may serve as an independent drought indicator (Hobbins et al., 2016). Recently, the evaporative demand drought index (EDDI) based solely on the PET is used to analyze and monitor flash droughts (McEvoy et al., 2016). However, EDDI only considers PET and thus is inappropriate for regions with non-constraining soil moisture conditions, e.g. humid regions, given that positive PET anomaly is not representative of actual drought conditions (Vicente-Serrano et al., 2018).

The SAPEI relies on the precipitation and potential evapotranspiration. There are generally available observational precipitation and datasets for calculating potential evapotranspiration in most countries around the world. Therefore, SAPEI can be directly calculated using observed meteorological datasets, and the calculation process is simple. In addition, it has multiple time scales, and the long-time scale SAPEI is sensitive to soil moisture variation. It is commonly accepted that drought is a multiscale phenomenon. The time scale over which water deficits accumulate becomes extremely important, and it functionally separates hydrological, agricultural, and other droughts. Drought indices must be associated with a specific time scale to be useful for monitoring and managing different usable water resources (Vicente-Serrano et al.,

2010). Overall, the SAPEI meets the requirements of a drought index, given the fact that it shows reliable and robust ability for drought analysis and monitoring. Like the SPEI and SPI, SAPEI includes multiple time scales (3-, 6-, 9-, and 12- month) to monitor droughts at monthly resolution. However, SAPEI has the advantage over SPEI regarding sub-monthly drought monitoring. Such an index could help fill a gap between science and applications in that it would be operationally tractable for detecting and monitoring both short-term and sustained droughts.

We have added discussion on the added value of SAPEI compared with soil moisture indices in Lines 419-430.

#### Reference:

- Mishra, A. K., & Singh, V. P. (2010). A review of drought concepts. *Journal of hydrology*, 391(1-2), 202-216.
- Hobbins, M. T., Wood, A., McEvoy, D. J., Huntington, J. L., Morton, C., Anderson, M., & Hain, C. (2016). The evaporative demand drought index. Part I: Linking drought evolution to variations in evaporative demand. *Journal of Hydrometeorology*, 17(6), 1745-1761.
- McEvoy, D. J., Huntington, J. L., Hobbins, M. T., Wood, A., Morton, C., Anderson, M., & Hain, C. (2016). The evaporative demand drought index. Part II: CONUS-wide assessment against common drought indicators. *Journal of Hydrometeorology*, 17(6), 1763-1779.
- Vicente-Serrano, S. M., Beguería, S., López-Moreno, J. I., Angulo, M., & El Kenawy, A. (2010). A new global 0.5 gridded dataset (1901–2006) of a multiscalar drought index: comparison with current drought index datasets based on the Palmer Drought Severity Index. *Journal of Hydrometeorology*, 11(4), 1033-1043.
- Vicente-Serrano, S. M., Miralles, D. G., Domínguez-Castro, F., Azorin-Molina, C., El Kenawy, A., McVicar, T. R., ... & Peña-Gallardo, M. (2018). Global assessment of the Standardized Evapotranspiration Deficit Index (SEDI) for drought analysis and monitoring. *Journal of Climate*, 31(14), 5371-5393.

Reviewer (10): There are too many references to the supplementary material throughout the text. I suggest the authors reevaluate the necessity for each of the figures and come up with a set that is crucial to the story. This is not a research letter, there is more than enough space.

Author's reply (10): Thank you for your comments and suggestions. The supplementary materials mainly involve the metrics for selecting copula, and assessment of SAPEI/SCDHI ability to monitor monthly drought/compound dry-hot

conditions using real-world typical events. These analyses are necessary but not essential, so placing them in the supplementary material without adding manuscript space. If we remove these materials, the ability of the two indices to monitor monthly drought/dry-hot conditions could not be verified.

So, we would like to keep them, but have selected the essential panels and reduced the content related to supplementary materials. Please see Lines 348-361 and 376-387.

Reviewer (11): Line 462. If a hot index is based on absolute temperature, it seems trivial that places that are closer to the equator at low altitudes have the largest probability of a hot event. Can you explain more about the location where the outcome surprised you, or where new insights were found?

Author's reply (11): Thank you for your comment and suggestion.

In this study, the STI representing the hot condition is calculated by the temperature variation within a specific grid point (similar to common drought indices). For example, with respect to one certain grid point, the 1 January STI are computed on the 1 January temperature datasets observed during 1961-2018 at each grid point. In other words, the hot index (STI) is not affected by regional location and are only related to its changes within the grid point. Hot events are always only hot relative to the local climatology.

In addition, the Figure 11 shows the characteristics (e.g., frequency) of the compound dry-hot events. Though the compound dry-hot event is closely related to the extreme temperature, it reflects the concurrent dry and hot conditions. Extreme temperature is more frequent in some regions, but there may be relatively less compound dry-hot events due to less droughts.

In this study, we found that a high frequency of compound events was detected in southern China, and the events generally lasted about 25 days (Fig. 11a). The occurrence of extreme climate (e.g. high temperature, low humidity, and sunny skies) can appear within a short period without resulting in long-lasting compound events, but rather, short-term droughts and heatwave lasting a few weeks (Mo and Lettenmaier, 2015; Zhang et al., 2019). Previous studies state that short-term dry and hot events occur more frequently in southern regions than in other parts of China (Otkin et al., 2018; Wang et al., 2016). South China is a humid region where evapotranspiration is mainly controlled by energy supply because soil moisture is usually sufficient. The evaporation demand could increase significantly during a short period when strong, transient



meteorological changes occur. Through influencing evapotranspiration variation, short-term meteorological variables (e.g., solar radiation and sunshine duration) are considered an important factor in drought and hot concurrences. For instance, the largely increase in sunshine duration due to clear sky create excessive evapotranspiration, which in turn decrease soil moisture. More surface sensible heat fluxes are transferred to the near-surface atmosphere to further increase air temperatures and makes precipitation rare. These land-atmosphere interactions altogether create favorable conditions for concurrent drought and hot. Therefore, concurrent dry-hot events are likely to occur in south China.

We have added discussion on why southern China experience more compound dry-hot events. Please see Lines 547-560.

#### Reference:

- Mo, K. C., & Lettenmaier, D. P. (2015). Heat wave flash droughts in decline. *Geophysical Research Letters*, 42(8), 2823-2829.
- Otkin, J. A., Svoboda, M., Hunt, E. D., Ford, T. W., Anderson, M. C., Hain, C., & Basara, J. B. (2018). Flash droughts: A review and assessment of the challenges imposed by rapid-onset droughts in the United States. *Bulletin of the American Meteorological Society*, 99(5), 911-919.
- Wang, L., Yuan, X., Xie, Z., Wu, P., & Li, Y. (2016). Increasing flash droughts over China during the recent global warming hiatus. *Scientific reports*, 6, 30571.
- Zhang, Y., You, Q., Mao, G., Chen, C., & Ye, Z. (2019). Short-term concurrent drought and heatwave frequency with 1.5 and 2.0 C global warming in humid subtropical basins: a case study in the Gan River Basin, China. *Climate dynamics*, 52(7-8), 4621-4641.

Reviewer (12): Lines 485 and further: (a) How are the RCP scenarios computed in your index? This does not seem trivial to me, how is the input acquired? (b) It would be nice to know which of the observed increases in due to temperature alone and which due to more complex interactions?

Author's reply (12): Thank you for your questions and suggestion.

(a) To obtain the future climate scenarios data, we collect eight global climate models, including CanESM2, CNRM-CM5, CSIRO-Mk3.6, MIROC-ESM, MPI-ESM-LR, BCC-CSM1-1, IPSL-CM5A-LR, and MRI-CGCM3, to project the future climate conditions. These global climate models exhibit good performance to simulate the key features of precipitation and temperature in China. We obtained climate

variables (i.e., precipitation, temperature, relative humidity, wind speed, and shortwave and longwave radiations) for the future periods for the three Representative Concentration Pathways (RCPs) including RCP 2.6 (low emission scenario), RCP 4.5 (moderate emission scenario) and RCP 8.5 (high emission scenario). The bias-corrected climate imprint method, one of the delta statistical downscaling methods, was applied to downscale the climate model output to same resolution as the observations. Using the downscaling datasets, the SCDHI was computed, and was used to analyze future compound dry-hot events.

We have clarified these points in Lines 201-204.

(b) That is a good suggestion. We have calculated the future SCDHI considering only temperature change, and then this SCDHI will be compared to historical reference. Finally, this result has been compared with the Figure 12 in first-round manuscript to illustrate future changes in characteristics of the compound dry and hot events due to temperature change.

The detailed analyses are shown in Lines 594-620 and Figure 12 in revised manuscript.

1 **A standardized index for assessing sub-monthly compound**  
2 **dry and hot conditions: application in China**

3 Jun Li<sup>1</sup>, Zhaoli Wang<sup>1,2</sup>, Xushu Wu<sup>1,2,\*</sup>, Jakob Zscheischler<sup>3,4</sup>, Shenglian Guo<sup>5</sup>,  
4 Xiaohong Chen<sup>6</sup>

5 <sup>1</sup> *School of Civil Engineering and Transportation, State Key Laboratory of Subtropical*  
6 *Building Science, South China University of Technology, Guangzhou 510641, China.*

7 <sup>2</sup> *Guangdong Engineering Technology Research Center of Safety and Greenization for*  
8 *Water Conservancy Project, Guangzhou 510641, China.*

9 <sup>3</sup> *Climate and Environmental Physics, University of Bern, Sidlerstrasse 5, 3012 Bern,*  
10 *Switzerland.*

11 <sup>4</sup> *Oeschger Centre for Climate Change Research, University of Bern, Bern, Switzerland.*

12 <sup>5</sup> *State Key Laboratory of Water Resources and Hydropower Engineering Science,*  
13 *Wuhan University, Wuhan 430072, China.*

14 <sup>6</sup> *Center for Water Resource and Environment, Sun Yat-Sen University, Guangzhou*  
15 *510275, China*

16 *\*Correspondence: xshwu@scut.edu.cn.*

17

18 **Abstract:** Compound dry ~~and~~ hot conditions pose large impacts on ecosystems and  
19 society worldwide. A suite of indices are proposed for the assessments of droughts and  
20 heatwaves previously, yet there is no index available for incorporating the joint  
21 variability of dry and hot conditions at sub-monthly scale. Here, we introduce a daily-  
22 scale index, termed as the standardized compound drought and heat index (SCDHI), to  
23 measure the intensity of compound dry and hot conditions. SCDHI is based on the daily  
24 drought index (the standardized antecedent precipitation evapotranspiration index  
25 (SAPEI)) and the ~~Standardized~~ standardized Temperature ~~temperature~~ Index ~~index~~  
26 (STI) and a joint probability distribution method. The new index is verified against real-  
27 world compound dry and hot events and the related observed vegetation impacts in  
28 China. SCDHI can not only monitor the long-term compound dry and hot events, but  
29 also capture such events at sub-monthly scale and reflect the related vegetation activity  
30 impacts. The identified compound events generally persisted for 25-35 days and the  
31 southern China suffered from compound events most frequently. In future, the  
32 frequency, duration, severity and intensity of compound events increase throughout  
33 China in response to anthropogenic climate change, of which the frequency would  
34 generally increase by 1-3 times and the duration and severity increase by 50%; under  
35 largest emission scenario, duration, severity, and frequency across Midwest China  
36 increase by at least 3 times. ~~, independent of the emission scenarios.~~ The new index can  
37 provide a new tool to quantify sub-monthly characteristics of compound dry and hot  
38 events, conducive to the timely monitoring of their initiation, development, and decay  
39 which are vital for decision-makers and stake-holders to release early and timely  
40 warnings.

41 **Keywords:** compound event; SCDHI; SAPEI; sub-monthly scale; China

42

## 43 **1 Introduction**

44 Compound dry ~~and~~ hot event (~~CDHE~~) have been observed for all continents in  
45 recent decades (Hao et al., 2019; Mazdiyasi and AghaKouchak, 2015; Manning et al.,  
46 2019; Sutanto et al., 2020). The frequent ~~CDHEs~~ compound dry-hot events have led to  
47 more devastating impacts on natural ecosystems and human society than individual  
48 events (Zscheischler et al., 2014, 2018; Chen et al., 2019; Hao et al., 2018a). ~~For~~  
49 ~~example, Russia was simultaneously struck by an unprecedented drought and hot in the~~  
50 ~~summer of 2010, which caused large-scale crop failures, wildfires, and human mortality~~  
51 ~~(Zscheischler et al., 2018)~~. Unfortunately, the extreme droughts and hots are expected  
52 to occur more frequently in the coming decades under global warming, which  
53 potentially results in more compound events in many parts of the world, especially for  
54 wet and humid regions (Wu et al., 2020; Swain et al., 2018, Zscheischler and  
55 Seneviratne, 2017a). Therefore, understanding such events are of crucial importance to  
56 provide the most fundamental information to help disaster mitigation.

57 Much effort has been made to study the compound events in recent years. Utilizing  
58 different thresholds to define the concurrent climate extremes for a specific period, the  
59 frequency of compound events has ~~received~~ received a great deal of attention (Wu et  
60 al., 2019; Zhang et al., 2019). Although this approach ~~can~~ can detect compound event  
61 occurrence, it fails to quantitatively measure compound event characteristics such as  
62 duration, severity, and intensity, and is inconvenient for comparison of compound event  
63 characteristics through different climates (Wu et al., 2020). Therefore, to overcome  
64 these shortages, several joint climate extreme indices have been proposed for analyzing  
65 the characteristics of the compound events. ~~For example, the climate extreme index~~  
66 ~~integrated by temperature and soil moisture extremes was presented for monitoring~~  
67 ~~trends in multiple types of climate extremes across large regions, and has been~~

68 employed to assess changes in spatial extent (Gallant et al., 2014). In recent years,  
69 several compound dry and hot indices have been developed. For example, Specifically,  
70 the Standardized standardized Dry dry and Hot hot Index index based on the ratio of  
71 the marginal probability distribution functions of precipitation and temperature was  
72 proposed to measure the extreme degree of a compound drought and hot extreme event  
73 (Hao et al., 2018). Hao et al. (2019, 2020) recently proposed the Standardized  
74 standardized Compound compound Event event Indicator indicator (SCEI) and  
75 compound dry-hot index to assess the severity of compound dry and hot events by  
76 joining the marginal distribution of Standardized standardized Precipitation  
77 precipitation Index index (SPI) and Standardized standardized Temperature  
78 temperature Index index (STI) using the copula theory. These two joint indices provide  
79 useful tools to improve our understanding of the frequency, spatial extent and severity  
80 of the compound dry-hot event. However, they are inevitably subjected to some  
81 shortcomings including the fixed monthly scale and the disregard of evapotranspiration,  
82 which may limit their use in monitoring the detailed evolution of compound dry and  
83 hot events.

84 With the occurrence of extreme climate (e.g. high temperature, low humidity, and  
85 sunny skies), droughts can evolve rapidly (~~Chen et al., 2019~~; Koster et al., 2019; ~~Mo~~  
86 ~~and Lettenmaier, 2015~~; Otkin et al., 2018; Yuan et al., 2019; Li et al., 2020a). Such  
87 extreme weather can appear within a short period without resulting in long-lasting  
88 compound events, but rather, short-term droughts and heatwaves lasting a few weeks  
89 or even days (Mo and Lettenmaier, 2016; Zhang et al., ~~2017~~2019). Severe concurrent  
90 drought and heat can suddenly strike a region with a relatively short duration when  
91 extreme weather anomalies persist over the same region (Röthlisberger and Martius,  
92 2019; Wang et al., 2016). Concurrent short-term drought and hot can pose greater

93 potential socio-economic risks because the combination of these events can exacerbate  
94 their respective environmental and societal impacts (Kirono et al., 2017; Schumacher  
95 et al., 2019; Sedlmeier et al., 2018). Specifically, even short-term concurrent dry and  
96 hot extremes can lead to significant agricultural loss if they occur within sensitive stages  
97 in crop development such as emergence, pollination, and grain filling (Zhang et al.,  
98 2019). ~~For example, a strong precipitation deficit along with record high temperatures~~  
99 ~~have led to severe impacts during May and early June in 2012 across the central U.S.~~  
100 ~~(Ford and Labosier, 2017; Otkin et al., 2013). Such short term concurrent dry and hot~~  
101 ~~events regularly inflict widespread agricultural crop losses and drastically cut down~~  
102 ~~livestock population, making it one of the most costly natural hazards in the U.S. history~~  
103 ~~at tens of billions of economic losses (Anderson et al., 2016; Otkin et al., 2019).~~ Under  
104 climate change, short-term concurrent dry and hot extremes are expected to increase  
105 (especially for humid regions), potentially causing substantial damage to natural  
106 ecosystems and society (Li et al., 2020b; Sun et al., 2019). To improve understanding  
107 of such short-term compound events and make early and timely warnings, decision-  
108 makers and stakeholders require more detailed information such as the start time,  
109 severity, and the projected tendency in the coming days rather than the average state at  
110 a fixed monthly scale. Correspondingly, sub-monthly scale indices for characterizing  
111 short-term compound dry and hot events are needed. In addition, ~~t~~Through the influence  
112 of evapotranspiration, short-term meteorological variables (e.g., temperature and  
113 radiation ~~solar radiation and sunshine duration~~) are considered an important factor in  
114 drought and heatwave concurrences (James et al., 2010). ~~For example, the largely~~  
115 ~~increase in sunshine duration due to clear sky creates excessive evapotranspiration,~~  
116 ~~which in turn decreases soil moisture (Ford et al., 2015). More surface sensible heat~~  
117 ~~fluxes is transferred to the near surface atmosphere to further increase air temperatures~~

118 ~~and prohibit precipitation (Miralles et al., 2019; Vogel et al., 2018). Together, these~~  
119 ~~land-atmosphere interactions create favorable conditions for concurrent drought and~~  
120 ~~heatwaves (Mo and Lettenmaier, 2016; Otkin et al., 2018).~~ Thus, the development of a  
121 compound drought and heat index should consider other important drought/hot-related  
122 factors including temperature and precipitation~~including temperature and precipitation~~  
123 (e.g. evapotranspiration).

124 The complexity of compound events makes it an unusual task to develop a simple  
125 and robust index to quantify their past and future changes (Zscheischler et al., 2020). A  
126 suite of indices are proposed for the assessments of droughts and heatwaves previously,  
127 yet there is no index available for incorporating the joint variability of dry and hot  
128 conditions at sub-monthly scale. Here we aim to formulate a compound drought and  
129 heat index, called the standardized compound drought and heat index (SCDHI), for  
130 monitoring and analyzing compound dry and hot events at sub-monthly scale. To  
131 achieve this aim, we combine a daily scale drought index, the standardized antecedent  
132 precipitation evapotranspiration index (SAPEI), which simultaneously considers  
133 precipitation and potential evapotranspiration, with a daily scale standardized  
134 temperature index (STI). We investigate the characteristics such as frequency, duration,  
135 severity, and intensity of compound dry-hot events during the historical (1961-2018)  
136 period and project their changes in China for the future (2050-2100) under different  
137 emission scenarios. This index can provide a new tool to quantify the characteristics of  
138 compound dry-hot event, and can monitor the compound dry-hot event at multiple time  
139 scale (e.g., daily, weekly and monthly) to provide detailed information on their  
140 initiation, development, decay, and trends.



## 141 2 Methods

### 142 2.1 data

143 Daily meteorological datasets covering 1961 to 2018 were collected from 2239  
144 observational stations across the non-arid region in China (Fig. 1), which include  
145 precipitation ( $P$ ), maximum air temperature ( $T_{\max}$ ), mean air temperature ( $T_{\text{men}}$ ),  
146 minimum air temperature ( $T_{\min}$ ), relatively humidity ( $RH$ ), wind speed ( $WS$ ), and  
147 sunshine duration. All of these meteorological data with strict quality control are  
148 available from the China Meteorological Administration (<http://cdc.nmic.cn/home.do>)  
149 and the Resources and Environmental Science Data Center, Chinese Academy of  
150 Sciences (<http://www.resdc.cn/Default.aspx>). ~~The kriging method was applied to~~  
151 ~~interpolate these~~ The observational station data were interpolated into  $0.25 \times 0.25^\circ$   
152 gridded data by kriging method, as it yields higher interpolation accuracy than the  
153 other commonly used methods, e.g., ordinary nearest neighbor and inverse distance  
154 weighting (Liu et al., 2016). In this study, we only focus the non-arid region in China,  
155 because of three reasons: (1) replenishment of water resources across Chinese arid  
156 region is mainly from melted glacial or perennial frozen soil, but not from precipitation.  
157 The statistical drought indices are usually limited its role in revealing drought in such  
158 complex situation; (2) meteorological observations in Chinese arid regions are too  
159 scarce to conduct robust analysis (Wu et al., 2007; Xu et al., 2015); (3) from a practical  
160 perspective, calculating climate extreme indices across arid region with large-scale  
161 desert regions is less meaningless (Tomas-Burguera et al., 2020).

162 The two commonly used indices (i.e., monthly Palmer dDrought sSeverity iIndex  
163 (PDSI) and Sandardized standardized precipitation eEvapotranspiration iIndex (SPEI)  
164 were employed for comparison. PDSI and SPEI were computed from the same

165 meteorological data described above. The conventional PDSI was empirically derived  
166 using the meteorological data of the central USA with its semi-arid climate. The  
167 portability of the conventional PDSI is thus relatively poor (Liu et al., 2017). In this  
168 study, PDSI was calculated according to the China national standard of classification  
169 of meteorological drought with standard number of GB/T 20481-2017. The PDSI  
170 ~~calculation procedure of this standard~~ was built based on long-term meteorological data  
171 of in-situ stations evenly distributed around China, hence well monitor drought in China  
172 (Zhong et al., 2019a), and the detailed calculation on the PDSI is shown in  
173 supplementary materials. The 0.25°-daily root zone (0 - 100 cm) soil moisture dataset  
174 obtained from Community Land Model (~~CLM~~) of the Global Land Data Assimilation  
175 System (~~GLDAS~~) was also used in this study. Community Land Model product does  
176 not have explicit vertical levels, instead soil moisture is represented in surface (0-2cm),  
177 and root zone (0-100cm). Root zone soil moisture is chosen over the surface soil  
178 moisture on account of its appositeness to characterize drought, low noise relative to  
179 surface soil moisture (Hunt et al., 2009; Osman et al., 2020). The dataset from 1961 to  
180 2014 were downloaded from the Goddard Earth Sciences Data and Information  
181 Services Center (Rodell et al., 2004). The ~~GLDAS-CLM~~ soil moisture dataset from  
182 Community Land Model can captures dry and wet conditions in China well (Bi et al.,  
183 2016; Feng et al., 2016). To avoid the effect of seasonality, the soil moisture was fitted  
184 by Gamma probability distribution, and then was standardized by normal quantile  
185 transformation. In addition, 8-day leaf area index (~~LAI~~) of the MOD15A2H from 2003  
186 to 2018 were collected. These data were resampled to 0.25° spatial resolution, and then  
187 the Z-score was used to calculate the leaf area index~~LAI~~ anomalies.

188 We further used eight global climate models from the Coupled Model  
189 Intercomparison Project Phase 5 (<https://esgf.llnl.gov/>) (Taylor et al., 2012), including

190 CanESM2, CNRM-CM5, CSIRO-Mk3.6, MIROC-ESM, MPI-ESM-LR, BCC-CSM1-  
191 1, IPSL-CM5A-LR, and MRI-CGCM3, were used to project the future climate  
192 conditions. These GCMs global climate models exhibit good performance to simulate  
193 the key features of precipitation and temperature in China (Jiang et al., 2016; Yang et  
194 al., 2019). We obtained daily climate variables (i.e., precipitation, temperature,  
195 relatively humidity, wind speed, P, T<sub>max</sub>, T<sub>min</sub>, T<sub>men</sub>, WS, RH, and shortwave and  
196 longwave radiations) for the historical (1961-2005) and future (2030-2050-2100)  
197 periods for the three Representative Concentration Pathways (RCPs) including RCP 2.6  
198 (low emission scenario), RCP 4.5 (moderate emission scenario) and RCP 8.5 (high  
199 emission scenario). All of the global climate models GCM outputs were based on the  
200 first ensemble member of each model, referred to as *r1i1p1* in all of the experiments.  
201 In this study, the bias-corrected climate imprint method, one of the delta statistical  
202 downscaling methods, was used to downscale the global climate models outputs to a  
203 spatial resolution of 0.25° (Werner and Cannon, 2016). The detailed information on  
204 these global climate models GCMs is shown in Table S1.

## 205 **2.2 Development of SCDHI**

206 The SCDHI is a compound drought and heat index based on a daily drought index  
207 and the Standardized Temperature Index (STI), which is computed in a similar fashion  
208 as the Standardized Precipitation Index (Zscheischler et al., 2014). The calculation of  
209 daily STI is similar to monthly STI, but for standardizing daily temperature. For  
210 example, with respect to one certain grid point, the 1 January STI are computed on the  
211 1 January temperature datasets observed during 1961-2018 at each grid point. We firstly  
212 formulated a daily scale drought index, i.e. the standardized antecedent precipitation  
213 evapotranspiration index (SAPEI), by considering both precipitation and potential  
214 evapotranspiration PET. The Penman-Monteith method is used to calculate the potential

215 evapotranspiration, requiring temperature, relative humidity, wind speed, and  
216 sunshine duration. Afterward, the joint distribution method was employed to compute  
217 the SCDHI.

### 218 **2.2.1 Formulation of daily-scale drought index**

219 Li et al. (2020b) have proposed the daily-scale drought index (SAPEI) that  
220 considers both precipitation and potential evapotranspiration~~PET~~. However, the  
221 primary limitation of this index is that it has a fixed temporal scale and cannot reflect  
222 the dry and wet condition at different time scales. Hence, in this study, we developed  
223 the multiple time scale (i.e., 3-, 6-, 9-, and 12-month) daily drought index. Here, we  
224 followed the same nomenclature proposed by Li et al. (2020b) to refer to a daily  
225 standardized drought index (SAPEI) based on precipitation and potential  
226 evapotranspiration~~PET~~. SAPEI is simple to calculate, and uses the antecedent  
227 accumulative differences between precipitation and potential evapotranspiration~~PET~~ to  
228 represent the dry and wet condition of the current day. The calculation procedure is  
229 described below.

230 The Penman-Monteith method (Allen et al., 1998) was firstly used to compute  
231 potential evapotranspiration~~PET~~. With a value for potential evapotranspiration~~PET~~, the  
232 daily difference between precipitation and potential evapotranspiration~~PET~~ was  
233 calculated to reveal climatic water balance (precipitation minus potential  
234 evapotranspiration~~PET~~). To reflect dry and wet conditions of the day, the antecedent  
235 water surplus or deficit (~~D~~)(WSD) was calculated through the following equations:

$$WSD = \sum_{i=1}^n (P - PET)_i \quad (1)$$

236 Where ~~n~~ is the number of previous days, PET represents the potential  
237 evapotranspiration, and P represents precipitation.

238 The  $WSD_{\mathcal{D}}$  values can be aggregated at different time scales, such as 3, 6, 9 months,  
239 and so on. A probability distribution was used to fit the daily time series  $WSD_{\mathcal{D}}$ . Given  
240 that different probability distributions may cause differences in drought indices (Stagge  
241 et al., 2015), to select the most suitable distribution, several commonly probability  
242 distributions including the general extreme value, log-logistic, lognormal, Pearson III,  
243 generalized Pareto, exponential, and normal distributions, should be used to fit the  
244  $WSD_{\mathcal{D}}$  series. In the study of Li et al. (2020b), Shapiro-Wilk and Kolmogorov-  
245 Smirnov (KS) test have been used applied for optimal probability distribution selection  
246 by comparing the empirical probability distribution with a candidate theoretical  
247 probability distribution. They suggested that the log-logistic distribution is more  
248 suitable for SAPEI. Moreover, previous researches have demonstrated that the log-  
249 logistic distribution is suitable for standardizing drought indices, e.g. SPEI (Vicente-  
250 Serrano et al., 2010). Therefore, we chose the log-logistic distribution to compute  
251 SAPEI. Once the daily  $WSD_{\mathcal{D}}$  series were fit to a probability distribution, cumulative  
252 probabilities of the  $WSD_{\mathcal{D}}$  series were obtained and transformed to standardized units  
253 (SAPEI) using the classical approach of Barton et al. (1965).

### 254 2.2.2 Construction of SCDHI

255 The SCDHI was established through copula theory ([a brief introduction on copula](#)  
256 [theory is shown in supplementary materials](#)), which can combine the candidate  
257 variables into one numerical expression. This approach not only realizes a projection  
258 from multiple dimensions to [a single dimension](#)~~a single dimension~~, but also the  
259 marginal distributions of the candidate variables combined with their original structures  
260 can be fully preserved within the constructed joint distribution. Hence, the copula-based  
261 index provides an objective description of the compound events (Hao et al., 2018b;  
262 Terzi et al., 2019).

263 There are many copula families available, which have widely been used for jointing  
 264 bivariate distributions (Terzi et al., 2019; Zhang et al., 2018). Among them, Clayton,  
 265 Gumbel, Normal, T, and Frank copula perform well for jointing bivariate  
 266 hydrometeorological variables (Ayantobo et al., 2018; Liu et al., 2019), and thus were  
 267 employed to establish the bivariate joint probability distribution in this study. Assuming,  
 268 the two random Gaussian variables  $X$  and  $Y$  representing SAPEI and STI,  
 269 respectively, the compound dry-hot event CDHE can be identified as one variable  $X$   
 270 lower than or equal to a threshold  $x$ , and the other variable  $Y$  higher than a threshold  
 271  $y$  at the same time. The joint probability  $P$  of the compound dry-hot event CDHE can  
 272 then be expressed as:

$$p = P(X \leq x, Y \geq y) = u - c(u, v) \quad (2)$$

273 where  $u$  was the  $X$  marginal distribution, and  $c(u, v)$  was the joint probability  
 274 distribution.

275 This joint cumulative probability  $P$  could be treated as an indicator, where smaller  
 276  $P$  values denote more severe condition of compound dry-hot event CDHE. However,  
 277  $P$  to the given marginal sets,  $P$  values in different seasons or areas reflected different  
 278 conditions and are thus not comparable. Hence, the joint probability  $P$  was  
 279 transformed to a uniform distribution by fitting a distribution  $F$ , which was then  
 280 standardized as an indicator to characterize compound dry-hot events CDHEs. Once  
 281 the  $P$  series at each day were fitted to a copula, the  $P$  series were transformed to

282 standardized units. SCDHI can be estimated by taking the inverse of joint cumulative  
283 probability (p) as:

$$SCDHI = \varphi^{-1}(F(P(X \leq x, Y \geq y))) \quad (3)$$

284 where  $\varphi$  is the standard normal distribution function. the distribution  $F$  was  
285 estimated based on the Yeo-Johnson transformation formula (Yeo and Johnson, 2000).

286 Following the categories of compound dry and hot conditions as suggested by (Wu  
287 et al., 2020), we defined five categories of compound dry and hot conditions, including  
288 abnormal, light, moderate, heavy and extreme compound drought-hot, as shown in  
289 Table 1.

290 We used Akaike information criterion (~~AIC~~), Bayesian information Criterion (~~BIC~~),  
291 and Kolmogorov-Smirnov ~~KS~~ statistics as goodness-of-fit measures to select an  
292 appropriate copula. These statistical measures have been commonly used for estimating  
293 the goodness of fit of a proposed cumulative distribution function to a given empirical  
294 distribution function (Liu et al., 2019; Terzi et al., 2019). The ~~AIC, BIC, and KS~~  
295 statistics of the three metrics are presented in Fig. S1-3. According to the evaluation  
296 metrics, ~~there was a good agreement between the empirical and parametric copulas.~~  
297 ~~Particularly, the performance of Frank copula slightly outweighed those of the other~~  
298 ~~three copulas. Therefore,~~ the Frank copula was utilized to establish the joint probability  
299 function and construct SCDHI in this study. Note that the SCDHI under three future  
300 scenarios is also used the Frank copula, while the parameters are assessed by future  
301 scenarios data. The SCDHI development was illustrated in Fig. S4.

302 Furthermore, to verify the ability of SCDHI to capture the compound dry and hot  
303 event, three verification metrics were used (i.e., probability of detection (~~POD~~), false  
304 alarm ratio (~~FAR~~), and critical success index (~~CSI~~)) (Winston and Ruthi, 1986 ~~Zhang et~~

305 [al., 2018](#)).

$$\text{Probability of detection} = \text{hit} / (\text{hit} + \text{miss}) \quad (4)$$

$$\text{Probability of detection} = \text{hit} / (\text{hit} + \text{miss})$$

$$\text{False alarm ratio} = \text{false alarm} / (\text{hit} + \text{false alarm}) \quad (5)$$

$$\text{Critical success index} = \text{hit} / (\text{hit} + \text{false alarm} + \text{miss}) \quad (6)$$

306 where *hit* (*H*) (~~Hit~~, observed drought-hot) refers to the number of grids when SAPEI  
307 and STI is subjected to ~~grade 1-4~~ grade 1 (G1) ~~— grade 4 (G4)~~ and SCDHI is subjected  
308 to ~~grade 1-4~~ G1-G4; *M* (~~Miss~~) denotes the number of grids when SAPEI and STI is  
309 between ~~grade 1-4~~ G1 to G4 and SCDHI is subjected to other grades than ~~grade 1-4~~ G1-  
310 G4; *F* (~~false~~ False alarm) denotes the number of grids when SAPEI and STI is  
311 subjected to other grades than ~~grade 1-4~~ G1-G4 but SCDHI is subjected to grades of  
312 grade 1-4 G1-G4.

### 313 **3 Results and Discussion**

#### 314 **3.1 Evaluation of SAPEI**

315 The SCDHI was established based on the STI and daily-scale drought index, i.e.,  
316 SAPEI. However, no previous studies have tested the (daily) drought monitoring  
317 performance of SAPEI. When developing a drought index, rigorous testing is required  
318 with respect to its applicability before it is applied in drought monitoring. Fig. 2 shows  
319 the spatial distributions of the correlations between SAPEI and SPEI/PDSI/soil  
320 moisture across China. The monthly mean SAPEI at 3-, 6-, 9- and 12-month scale all  
321 showed strong agreement with the SPEI in China, with correlation coefficients higher  
322 than 0.8 ( $p < 0.01$ ), indicating that the monthly SAPEI at multiple time scale calculated  
323 from the daily value could have the same capability of monthly drought monitoring as



324 SPEI. The 3-, 6-, 9- and 12-month SAPEI generally showed good correlation with PDSI,  
325 and 3-month SAPEI and PDSI generally correlate closely, with correlation coefficients  
326 higher than 0.6 ( $p < 0.01$ ), ~~while the 12-month SAPEI displayed weak correlation with~~  
327 ~~PDSI in south China~~. For daily SAPEI at ~~3~~12-month scale and soil moisture, a close  
328 correlation was detected in south and north China, while relatively weak correlation is  
329 found in ~~north~~Midwest China. The correlation between SAPEI and soil moisture  
330 increased in magnitude ~~and spatial extent~~ at time scales of ~~6~~3-12~~9~~ months. For 12-  
331 month SAPEI, mean correlation coefficient ~~was reached 0.5~~generally greater than 0.6  
332 ~~for a majority of whole~~ China. This phenomenon implied that the short-time scale  
333 SAPEI was more sensitive to precipitation change, and thus could be more suitable for  
334 meteorological drought, while the long-time scale (more than five month) SAPEI was  
335 more closely related to soil moisture and can be applied for agricultural drought  
336 monitoring. Overall, these analyses indicate that the SAPEI at daily and monthly scale  
337 showed reliability in drought monitoring.

338 To further test the drought monitoring performance of the SAPEI, typical drought  
339 events were chosen as case studies. During recent decades, several well-known large-  
340 scale drought events have hit China, including the droughts in winter of 2009 to spring  
341 of 2010, and in 2011 (Lu et al., 2014; Yu et al., 2019). In this study, the drought regimes  
342 during these events were taken as case studies to evaluate the drought monitoring  
343 performance of SAPEI at 3-~~and 6~~-month time scales (Sun and Yang, 2012). We firstly  
344 showed the monthly evolution of these events by the monthly mean SAPEI, SPEI, and  
345 PDSI, and then analyzed the daily evolution of drought in space and time in the most  
346 affected areas according to SAPEI and soil moisture.

### 347 **3.2.1 Drought events during 2009-2010**

348 ~~Fig. S5 illustrates the monthly changes in the 2009/10 drought monitored by the~~

349 ~~PDSI, SPEI, and SAPEI at 3- and 6-month scale.~~ As shown in Fig. S5, the monthly  
350 evolution in 2009/10 drought based on SAPEI was generally similar with that of SPEI  
351 and PDSI. This drought started to appear in most of China (except for the central and  
352 northeast China) in September 2009, and then persisted in most of China during  
353 October to December 2009; ~~during this period, drought conditions became more severe~~  
354 ~~in south China.~~ During January and April in 2010, severe drought persisted in southwest  
355 China~~The drought in north and east China gradually faded away during January and~~  
356 ~~March in 2010. In contrast, in southwest China (SWC) the drought intensity became~~  
357 ~~rather strong during the same period. The severe dry condition continued in SWC~~  
358 ~~during April in 2010,~~ while drought in the rest of China gradually disappeared in this  
359 period. After that, dry conditions in southwest China~~SWC~~ gradually relieved from May  
360 to June in 2010, but did not disappear. ~~The monthly drought evolution based on SAPEI~~  
361 ~~was generally similar with that of SPEI and PDSI.~~

362 Despite being located in the humid climate zone, southwest China~~SWC~~ suffered  
363 from exceptional drought during the autumn of 2009 to the spring of 2010 (Lin et al.,  
364 2015). During this drought, more than 16 million people and 11 million livestock faced  
365 drinking water shortages, with direct economic losses estimated at 19 billion yuan in  
366 southwest China~~SWC~~ (Lin et al., 2015). We selected this event in southwest China~~SWC~~  
367 as the first case study, and reveal detailed spatial and temporal change of this event at  
368 daily scale based on SAPEI and soil moisture (Fig. 3 and 4). During September 1 to 30  
369 of 2009, the drought started to appear in the region, and dry conditions became worse  
370 and spread throughout nearly the entire southwest China~~SWC~~ from October 1 to  
371 November 15 of 2009. Severe dry conditions then stayed in the region for 152 days  
372 from November 15 to April 15 of 2010, with high intensity. Afterwards, severe drought  
373 was gradually relieved from April 15 to June 15. The drought diminished over time in

374 most parts of southwest China by the end of June.

### 375 3.2.2 Drought events in 2011

376 ~~The monthly changes in the 2011 drought is illustrated in~~ As shown in Fig. S6. The  
377 ~~2011 drought~~ monthly pattern monitored by SAPEI are generally consistent ~~shows a~~  
378 ~~good agreement~~ with those by SPEI and PDSI. ~~More specifically,~~ ~~†~~ The drought mainly  
379 started in north China in January, while in March it spread to most of China, ~~and severe~~  
380 ~~dry conditions persisted in most areas during April to May,~~ ~~and drought conditions in~~  
381 ~~lower reaches of the Yangtze River basin became serious. In April to May, severe dry~~  
382 ~~conditions persisted in the middle and lower reaches of the Yangtze River Basin (MLR-~~  
383 ~~YRB), and extended from the YRB to southern China.~~ In August, the drought mainly  
384 moved ~~to southward~~ ~~westward and reached the edge of southwestern China.~~ Severe  
385 drought persisted in ~~the regions~~ ~~southwest China~~ during September and October, but it  
386 ~~then~~ gradually faded away ~~in November and December.~~ The results monitored by the  
387 SAPEI are generally consisted with the findings of Lu et al. (2014).

388 The 2011 drought event was particularly unusual in the ~~middle and lower reaches~~  
389 ~~of the Yangtze River Basin (MLR-YRB).~~ The MLR-YRB is generally in a wet  
390 condition, nevertheless, suffered its worst drought in the 50 years during the spring.  
391 The severe drought caused shortage of drinking water for 4.2 million people. 3.7 million  
392 hectares of crops were damaged or destroyed. Moreover, the heavy drought led to more  
393 than 1,300 lakes devoid of all water in Hubei province (Xu et al., 2015). The temporal  
394 and spatial evolution of this event in MLR-YRB described by daily SAPEI and soil  
395 moisture was shown in Fig. 5-6. The drought started to appear in the north part of the  
396 MLR-YRB in early February of 2011, and then gradually expanded to the whole MLR-  
397 YRB during early February and March 15. The severe drought condition persisted in  
398 this region for 78 days (from March 15 to May 31). Afterwards, there was a tendency

399 toward alleviating drought conditions, and most of MLR-YRB was under light and  
400 moderate drought conditions.

401 The previous detailed analysis showed that the SAPEI not only captures monthly  
402 characteristics of droughts, but also has the potential to track droughts at sub-monthly  
403 scale (Li et al., 2020b). Though the input data (including precipitation and potential  
404 evapotranspiration~~PET~~) of SAPEI are similar to SPEI, the rationale of the index is  
405 different from SPEI. It was calculated for each day and considers the water surplus or  
406 deficit of that day and the previous days. SPEI was commonly employed to monitor  
407 and analyze the monthly or longer-scale droughts (Vicente-Serrano et al., 2010). It thus  
408 may not be appropriate to apply the SPEI at shorter timescales (e.g., daily or weekly),  
409 because of the inherent problem in the construction of the index. Although SPEI gives  
410 a full and equal consideration to the water surplus or deficit in the period of the  
411 considered time scale, it does not consider the water surplus or deficit in the days before  
412 the period. If the scale is very short, this may cause problems. For a 7-day period, for  
413 example, if there is no precipitation during the period, it may be regarded as a drought  
414 period when compared with historical records (the method used by the SPEI); however,  
415 if there is a heavy precipitation just before the period, then the 7-day period probably  
416 remains wet and is unlikely to experience drought condition during such a short time.  
417 Previous studies have demonstrated the disadvantage of SPEI for short-time scale  
418 drought monitoring (Lu, 2009; Lu et al., 2014; Li et al., 2020b).

419 Soil moisture would be the most appropriate variable for agriculture drought  
420 monitoring and analyses (Mishra and Singh, 2010). However, there are few long-term  
421 and large-scale observational soil moisture datasets due to insufficient observation  
422 stations around the world, especially for developing regions, which limits its wide use  
423 in drought monitoring and analyses (Seneviratne et al., 2010). Thus, using

424 observational hydrometeorological datasets, the complex physical process models, such  
425 as the variable infiltration capacity model, are widely used to simulate the soil moisture  
426 (Liang et al., 1996; Xia et al., 2018). However, running such models requires highly  
427 trained personnel not usually available at local agencies. In addition, when the model  
428 is used locally, it generally needs to be calibrated and verified by observational soil  
429 moisture and other hydrometeorological datasets (Xia et al., 2018; Zhou et al., 2019).  
430 This certainly limits the wide use of soil moisture as a drought indicator.

431 In summary, the SAPEI meets the requirements of a drought index, given the fact  
432 that it shows reliable and robust ability for drought analysis and monitoring. Like the  
433 SPEI, SAPEI includes multiple time scales (3-, 6-, 9-, and 12- month) to monitor  
434 droughts at monthly resolution and is relatively sensitive to soil moisture variation.  
435 However, SAPEI has the advantage over SPEI regarding sub-monthly drought  
436 monitoring. Such an index could help fill a gap between science and applications in that  
437 it would be operationally tractable for detecting and monitoring both short-term and  
438 sustained droughts.

### 439 **3.2 Evaluation of SCDHI**

440 The SCDHI was developed by ~~joining~~ joining the marginal distribution of the  
441 SAPEI and STI. Though the copula method has been widely utilized to connect  
442 bivariate distribution, the property of SCDHI in capturing compound dry-hot  
443 events CDHEs still needs to be tested. ~~Fig. 7 shows the spatial distributions of the~~  
444 ~~correlations between SCDHI and SAPEI/STI at daily scale across China. The SCDHI~~  
445 ~~all showed strong ( $p < 0.01$ ) correlation with the SAPEI at 3-, 6-, 9- and 12-month scale~~  
446 ~~in China, with correlation coefficients higher than 0.7. A significant correlation ( $p <$~~   
447 ~~0.01) was also detected between STI and SCDHI at multiple scales. Fig. 8-7 shows the~~  
448 spatial pattern ~~in~~ and density plot for probability of detection POD, false alarm ratio FAR,

449 and critical success indexCSI when the drought and hot events observed by SAPEI and  
450 STI, respectively, were related to compound drought-hot event detected by SCDHI at  
451 3-, 6-, 9- and 12-monthly scale. As shown in Fig. 87, probability of detectionPOD is  
452 close to 1 and false alarm ratioFAR is close to 0, implying that SCDHI can well detect  
453 in most of the areas where the droughts and hots were detected by SAPEI and STI. The  
454 values of critical success indexCSI indicated that the ratios of drought-hot affected  
455 areas detected by SAPEI and STI to the drought and hot areas detected by SCDHI were  
456 close to one. Overall, these analyses implied that SCDHI can well monitor droughts  
457 and hots that can be successfully captured by SAPEI and STI. The SCDHI thus detects  
458 compound dry-hot eventsCDHEs that are identified separately by the coincidence of  
459 low SAPEI and high STI. In addition, the SCDHI detects events that are very extreme  
460 in either the SAPEI or the STI and moderate in the other variable but thus still cause  
461 substantial damage (Zscheischler et al., 2017b). Furthermore, the SCDHI is able to  
462 quantify the magnitude of compound dry-hot eventsCDHEs.

463 To further test the drought-heat monitoring performance of the SCDHI, two typical  
464 CDHEcompound dry-hot events were chosen as case studies according to the Yearbook  
465 of Meteorological Disasters in China. One was a well-known compound drought and  
466 heatwave striking Sichuan-Chongqing region (SCR) with serious consequences during  
467 summer of 2006 (Wu et al., 2020), and the other occurred in southern China with  
468 adverse impacts on agriculture during July to September of 2009 (Wang et al., 2010).  
469 Sichuan-Chongqing regionSCR experienced continuous extreme temperature during  
470 mid-June to late August 2006. The duration and severity of this hot event were the worst  
471 on the historical record. Simultaneously, a heavy drought occurring once in 100 years  
472 hit this region. During this compound event, a population of over ten million was  
473 confronted with drinking water shortage, about twenty thousand km<sup>2</sup> of cropland

474 suffered serious losses, and more than one hundred times forest fire broke out. Local  
475 governments issued the most serious arid warning (Zhang et al., 2008). Thus, we take  
476 this typical drought-hot event as first case studies to evaluate the drought/hot  
477 monitoring performance of SCDHI. The monthly spatial pattern of this compound event  
478 in [Sichuan-Chongqing region](#)<sup>SCR</sup> is shown in Fig. S7, indicating that [Sichuan-](#)  
479 [Chongqing region](#)<sup>SCR</sup> during summer in 2006 experienced the moderate to extreme  
480 compound dry and hot conditions. Fig. 9-8 maps the spatial pattern of this compound  
481 event and its impact on vegetation from mid-June to late August. This event started to  
482 appear in [Sichuan-Chongqing region](#)<sup>SCR</sup> in mid-June 2006, and gradually spread  
483 throughout the whole [Sichuan-Chongqing region](#)<sup>SCR</sup> during June 19 to 26. The  
484 moderate dry-hot condition then persisted in the entire [Sichuan-Chongqing region](#)<sup>SCR</sup>  
485 from June 27 to August 5 in 2006, lasting for 40 days. The negative [leaf area index](#)<sup>LAI</sup>  
486 was scattered in some of the dry-hot affected areas. However, during August 6 to 21,  
487 the drought-hot event became even more severe with the onset of extremely hot  
488 temperatures, causing negative vegetation anomalies in most of the affected areas.

489 The monthly spatial pattern of another compound event in southern China during  
490 July to September of 2009 is shown in Fig. S8. Overall moderate to heavy compound  
491 dry and hot conditions are observed at monthly scale in this region. However, this event  
492 showed large fluctuation at weekly scale. According to the Yearbook, the hot event was  
493 divided into two periods: the first stage was from early to late July, and the other stage  
494 was from mid-August to early September. The fluctuating compound event caused  
495 adverse impact of crop pollination and grain filling, resulting in decrease of crop  
496 production. Fig. 10-9 maps the spatial pattern of this event and its impact on [leaf area](#)  
497 [index](#)<sup>LAI</sup>. In the first stage, the drought-hot event hit the most of southern China during  
498 July 5 to 12, and then it became severe in the west part of southern China during July

499 13 to 20. However, the hot event suddenly disappeared from July 21 to 28, leading to  
500 disappearance of the compound event in most of southern China (Fig. ~~910~~9a). Afterward,  
501 the compound event hit this region again from August 6 to 13, and its intensity was  
502 strong during August 14 to 21, with severe hot conditions. Subsequently, the intensity  
503 and spatial extent of the compound event faded away in north of southern China during  
504 August 22 to 29. This event extended to most of this region again from August 30 to  
505 September 14, with severe dry and hot condition. The compound events still stayed in  
506 this region from September 15 to 22 (Fig. ~~40b~~9b). Despite the short-term event, the  
507 anomalous change in vegetation was found in most of the dry-hot affected areas. This  
508 complex ~~event~~event indicates that monthly analyses of the event can provide an overall  
509 situation, but ~~is not be able to~~is not be able to capture the serious dry and hot conditions  
510 caused by a short-term extreme climate anomaly at shorter time scales. Though such  
511 short-term compound event only lasted for days or weeks, they lead to large agricultural  
512 losses if they occur within sensitive stages in crop development (i.e., pollination and  
513 grain filling) (Mazdiyasi and AghaKouchak, 2015). To provide timely information of  
514 the compound dry-hot eventsCDHEs, short-time scale analyses and monitoring of such  
515 events are essential.

516 Overall, the changes in these two compound dry-hot eventsCDHEs based on  
517 SCDHI are consistent with the national weather recordsreports  
518 (<http://www.weather.com.cn/zt/kpzt/>) and the Yearbook of Meteorological Disasters in  
519 China 2010 (<http://www.weather.com.cn/>). In summary, the SCDHI is able to robustly  
520 and reliably capture compound dry-hot eventsCDHEs at sub-monthly scale, and  
521 potentially provide a new tool to objectively and quantitatively analyze and monitor the  
522 characteristics of compound dry-hot eventsCDHEs in time and space.



### 523 3.3 Application

524 Here, we evaluate and compare the spatiotemporal variation of characteristics of  
525 compound dry-hot eventsCDHEs in China during growing season (April-September),  
526 because such events can easily cause adverse impact on agriculture and ecosystem  
527 during these periods (Hao et al., 2018; Wu et al., 2019). More precisely, the compound  
528 dry-hot eventsCDHEs during growing season (April-September) from 1961 to 2018  
529 were identified based on 3-month scale SCDHI and run theory (Wu et al., 2018), after  
530 which the frequency, duration, severity, and intensity of these events were analyzed (A  
531 specific case to identify compound dry-hot eventCDHE is shown in Fig. S9). We then  
532 projected their future characteristics changes under the RCP 2.6, 4.5 and 8.5 from 2050  
533 to 2100. Given that short-term concurrent dry and hot events generally persist for at  
534 least weeks (Otkin et al., 2018), only the events lasting for more than two weeks were  
535 considered in this study.

536 Fig. 4-10 shows spatial patterns of characteristics of the compound dry-hot events  
537 CDHEs. A high frequency of compound events was detected in southern China, with  
538 occurrence of every two years on average, in contrast, the eastern Tibet Plateau and  
539 northeast China experienced fewer compound events (Fig. 4-10a), which was  
540 generally consistent with the previous studies (Liu et al., 2020; Wang et al., 2016). The  
541 compound dry-hot eventCDHE generally lasted for about twenty-five to thirty-five  
542 days in most of China, while in east Tibet Plateau, the compound dry-hot eventCDHE  
543 persisted for less than twenty days (Fig. 4-10b). The severity and intensity of the  
544 compound dry-hot eventCDHE presented relatively similar patterns and showed that  
545 most of eastern China experienced high severity and intensity (Fig. 4-10c-d). Overall,  
546 southern China suffered more frequent compound dry-hot eventsCDHEs, with higher  
547 severity and intensity. Southern China is a humid region where evapotranspiration is

548 mainly controlled by energy supply because soil moisture is usually sufficient. For  
549 given adequate soil moisture in the initiation of drought, evaporative demand can  
550 increase rapidly during a short period when strong, transient meteorological changes  
551 (such as extreme temperature) occur, which in turn exhaust soil moisture to intensify  
552 drought conditions (Zhang et al., 2019, Otkin et al., 2018). Moreover, vegetation over  
553 south China is usually abundant and plants tend to suck more water from the soil when  
554 high temperatures occur, causing evapotranspiration increase and soil moisture decline  
555 (Li et al., 2020c; Wang et al., 2016). More surface sensible heat fluxes are thus  
556 transferred to the near-surface atmosphere to further increase air temperatures (Mo and  
557 Lettenmaier, 2015). These land-atmosphere interactions altogether cause the Bowen  
558 ratio to increase (Otkin et al., 2013, 2018), creating a favorable condition for short-term  
559 concurrency droughts and hots. Therefore, compound dry-hot event are more likely to  
560 occur in humid regions with higher severity and intensity.

561 Fig. 42-11 illustrates the spatial patterns of change in frequency, duration, severity,  
562 and intensity of the compound dry-hot eventsCDHEs under RCP 2.6, 4.5, and 8.5  
563 scenarios. According to Fig. 42a11a, the future (2050-2100) compound dry-hot  
564 eventCDHE frequency under three scenarios in most of east China will increase by  
565 about one to three times with respect to the reference period (1961-2018). Under RCP  
566 8.5 scenario, compound dry-hot eventCDHE at about 4% of the study region is expected  
567 to markedly increase by more than five times, which are scattered in the central to west  
568 parts of China. The duration of compound dry-hot eventCDHE across the east of the  
569 study region will mainly show an increase of about 0.5 times, while duration in mid-  
570 west China potentially increases by approximately 1.5 times under RCP 8.5 scenarios  
571 (Fig. 42b11b). The spatial pattern of future severity change is similar to the duration;  
572 severity in most of east China is projected to increase by about 0.5 time under three

573 scenarios; however, compound dry-hot eventCDHE severity over mid-west China is  
574 expected to more than triple under RCP 8.5 (Fig. 12e11c). The compound dry-hot  
575 eventCDHE intensity in most of the study region exhibits slight increase for all  
576 scenarios in comparison to the historical period.

577 ~~The cumulative density functions (CDFs) of the CHDE frequency, duration,~~  
578 ~~severity, and intensity in historical and future periods were quantified, and the result is~~  
579 ~~shown in Fig. 13. A substantial change in the values of CHDE frequency, duration,~~  
580 ~~severity, and intensity was detected between the historical and future projections. The~~  
581 ~~frequency, duration, severity, and intensity of CHDEs will intensify throughout the~~  
582 ~~China in future scenarios compared to the historical reference, as marked by the~~  
583 ~~movement towards the right side of the CDF curves. Specifically, the cumulative~~  
584 ~~probability of CDHE frequency is expected to increase by more than 80% under three~~  
585 ~~scenarios, compared with the 95<sup>th</sup> percentile value in historical period (Fig. 13a). The~~  
586 ~~cumulative probability of duration would increase by about 72% under RCP 8.5~~  
587 ~~scenario, while increment under RCP 2.6 scenario is relatively small (17%), in~~  
588 ~~comparison to the 95<sup>th</sup> percentile in reference period (Fig. 13b). The severity cumulative~~  
589 ~~probability project to increase by 42% and 53% under RCP 2.6 and 4.5 scenarios~~  
590 ~~respectively, but even increase by 88% under RCP 8.5 scenario (Fig. 13c). An increase~~  
591 ~~of at least 42% is observed in the intensity cumulative probability, compared with the~~  
592 ~~n reference period (Fig. 13d). Such an increase in the frequency, duration, severity, and~~  
593 ~~intensity of CDHEs across China could be a new normal in future.~~

594 Global warming is very likely to exacerbate the prevalence of the compound dry-  
595 hot eventsCDHEs (Pfleiderer et al., 2019). ~~Trends are often present in individual~~  
596 ~~variables (e.g., temperature, and precipitation), while can also occur in the dependence~~  
597 ~~between drivers of compound events, which consequently affects associated risks. The~~

598 ~~(negative) correlation between seasonal mean summer temperature and precipitation is~~  
599 ~~projected to intensify in many land regions, leading to more frequent extremely dry and~~  
600 ~~hot conditions (Kirono et al., 2017; Zscheischler and Seneviratne, 2017a).~~ The  
601 cumulative density functions of the future variations in compound dry-hot event  
602 characteristics considering only temperature and all variable changes were quantified,  
603 and the result is shown in Fig. 12. The frequency and intensity of the future variations  
604 in compound dry-hot event do not show large difference between two scenarios (i.e.,  
605 temperature and all variable changes), while duration and severity display great  
606 increase due to temperature variation, as marked by the movement towards the right  
607 side of the cumulative density curves. Increasing temperature could lead to remarkable  
608 increase evapotranspiration, and thus causing more surface sensible heat fluxes into  
609 atmosphere (Mo and Lettenmaier, 2015; Zhang et al., 2019). These land-atmosphere  
610 interactions altogether cause the Bowen ratio to increase (Otkin et al., 2013, 2018),  
611 creating a favorable condition for concurrence dries and hots. In short, temperature  
612 could be generally the primary factor increasing the compound dry-hot severity and  
613 duration (Cook et al., 2014). In addition, trends are often present in individual variables,  
614 while can also occur in the dependence between drivers of compound events, which  
615 consequently affects associated risks. The (negative) correlation between seasonal  
616 mean summer temperature and precipitation is projected to intensify in many land  
617 regions, leading to more frequent extremely dry and hot conditions (Kirono et al., 2017;  
618 Zscheischler and Seneviratne, 2017a), while variation in compound dry-hot event due  
619 to the complex interaction between climate variables is need further studied  
620 (Zscheischler et al., 2020). Overall, the frequency, severity, duration, and intensity of  
621 the compound dry-hot events CDHEs in China under global warming will increase  
622 significantly. Effective measures need to be implemented to decrease the CO<sup>2</sup>emissions

623 for compound dry and hot event mitigation.

## 624 **4 Conclusions**

625 Under global warming, the compound dry and hot event tends to more frequent and  
626 short-lived (i.e., days or weeks). Correspondingly, a compound drought and heat index  
627 should be able to monitor such event at sub-monthly scales in order to timely reflect  
628 dry and hot condition evolution. In this study, we developed a multiple time scale (e.g.,  
629 3-, 6-, 9, and 12- month) compound drought and heat index, termed as SCDHI, to  
630 monitor short-time (e.g., days or weeks) and long-time (e.g., months) compound event.  
631 This index was established based on the daily drought index (i.e., SAPEI) and  
632 Standardized Temperature Index (STI) using a joint probability distribution method.  
633 Using the SCDHI, we then quantitatively investigated the characteristics (i.e., frequency,  
634 intensity, severity, and duration) of the compound dry-hot eventCDHEs in China in  
635 historical period (1961-2018), and revealed how they would change in the future (2050-  
636 2100) under representative concentration pathway (RCP) 2.6, 4.5, and 8.5 scenarios.  
637 The main conclusions of this study are presented as follows: The SCDHI can well  
638 monitor simultaneous dries and hots detected by SAPEI and STI. The monthly SCDHI  
639 can provide an overall situation of the compound dry and hot conditions, but sub-  
640 monthly SCDHI can well capture fluctuation of simultaneous dries and hots within a  
641 month. It also can reflect the impact of the compound dry and hot event on vegetation  
642 anomalies. The SCDHI can offer a new tool to quantitatively measure the  
643 characteristics of the compound dry-hot eventCDHEs. It also can provide detailed  
644 information such as the initiation, development, decay, and tendency of the compound  
645 event for decision-makers and stakeholders to make early and timely warning. In the  
646 case study of the China, the southern China suffered more frequent the compound dry-  
647 hot eventCDHE, with higher severity and intensity. The compound dry-hot eventCDHE

648 mainly lasted for twenty-five to thirty-five days in China. The frequency, duration,  
649 severity, and intensity of compound events will intensify throughout the China in future.  
650 The frequency will increase by about one to three times with respect to the reference  
651 period. A region with fewer compound event (< 5) would exhibit a multi-fold (more  
652 than five times) increase in the future. The duration across east areas mainly increased  
653 by 0.5 times, while severity project to increase by about 0.5 to 1 times.

654  
655 **Data availability.** The observed meteorological datasets are available at  
656 <http://cdc.nmic.cn/home.do>. The CMIP5 datasets are available at <https://esgf.llnl.gov>.

657  
658 **Author Contributions.** Conceived and designed the experiments: JL, [WSSW](#).  
659 Performed the experiments: JL, [WSSW](#). Analyzed the data: JL. Wrote and edited the  
660 paper: JL, [WSSW](#), [WZZW](#), [ZJZ](#), [GSSG](#), [CXXC](#).

661  
662 **Competing interests.** The authors declare that they have no conflict of interest.

663

## 664 **Acknowledgement**

665 The research is financially supported by the National Natural Science Foundation  
666 of China (51879107, 51709117), the Guangdong Basic and Applied Basic Research  
667 Foundation (2019A1515111144), and the Water Resource Science and Technology  
668 Innovation Program of Guangdong Province (2020-29).

669

## 670 **References**

671 Allen, R. G., Pereira, L. S., Raes, D. and Smith, M.: Crop evapotranspiration:  
672 Guidelines for computing crop requirements, Irrig. Drain. Pap. No. 56, FAO,

673 doi:10.1016/j.eja.2010.12.001, 1998.

674 ~~Anderson, M. C., Zolin, C. A., Sentelhas, P. C., Hain, C. R., Semmens, K., Tugrul~~  
675 ~~Yilmaz, M., Gao, F., Otkin, J. A. and Tetrault, R.: The Evaporative Stress Index~~  
676 ~~as an indicator of agricultural drought in Brazil: An assessment based on crop yield~~  
677 ~~impacts, Remote Sens. Environ., doi:10.1016/j.rse.2015.11.034, 2016.~~

678 Ayantobo, O. O., Li, Y., Song, S., Javed, T. and Yao, N.: Probabilistic modelling of  
679 drought events in China via 2-dimensional joint copula, J. Hydrol., 559, 373–391,  
680 doi:10.1016/j.jhydrol.2018.02.022, 2018.

681 Barton, D. E., Abramovitz, M. and Stegun, I. A.: Handbook of Mathematical Functions  
682 with Formulas, Graphs and Mathematical Tables., J. R. Stat. Soc. Ser. A,  
683 doi:10.2307/2343473, 1965.

684 Bi, H., Ma, J., Zheng, W. and Zeng, J.: Comparison of soil moisture in GLDAS model  
685 simulations and in situ observations over the Tibetan Plateau, J. Geophys. Res.,  
686 doi:10.1002/2015JD024131, 2016.

687 Chen, L., Chen, X., Cheng, L., Zhou, P. and Liu, Z.: Compound hot droughts over  
688 China: Identification, risk patterns and variations, Atmos. Res., 227(May), 210–  
689 219, doi:10.1016/j.atmosres.2019.05.009, 2019.

690 ~~Cook, B. I., Smerdon, J. E., Seager, R., and Coats, S.: Global warming and 21 st century~~  
691 ~~drying. Climate Dynamics, 43(9-10), 2607-2627, 2014.~~

692 Feng, X., Fu, B., Piao, S., Wang, S., Ciais, P., Zeng, Z., Lü, Y., Zeng, Y., Li, Y., Jiang,  
693 X. and Wu, B.: Revegetation in China’s Loess Plateau is approaching sustainable  
694 water resource limits, Nat. Clim. Chang., doi:10.1038/nclimate3092, 2016.

695 ~~Ford, T. W. and Labosier, C. F.: Meteorological conditions associated with the onset of~~  
696 ~~flash drought in the Eastern United States, Agric. For. Meteorol.,~~  
697 ~~doi:10.1016/j.agrformet.2017.08.031, 2017.~~

698 Ford, T. W., McRoberts, D. B., Quiring, S. M. and Hall, R. E.: On the utility of in situ  
699 soil moisture observations for flash drought early warning in Oklahoma, USA,  
700 Geophys. Res. Lett., doi:10.1002/2015GL066600, 2015.

701 ~~Gallant, A. J. E., Karoly, D. J. and Gleason, K. L.: Consistent trends in a modified~~  
702 ~~climate extremes index in the United States, Europe, and Australia, J. Clim., 27(4),~~  
703 ~~1379–1394, doi:10.1175/JCLI-D-12-00783.1, 2014.~~

704 Hao, Z., Hao, F., Singh, V. P., Xia, Y., Shi, C. and Zhang, X.: A multivariate approach  
705 for statistical assessments of compound extremes, J. Hydrol., 565, 87–94,  
706 doi:10.1016/j.jhydrol.2018.08.025, 2018a.

707 Hao, Z., Hao, F., Singh, V. P. and Zhang, X.: Quantifying the relationship between  
708 compound dry and hot events and El Niño–southern Oscillation (ENSO) at the  
709 global scale, J. Hydrol., 567, 332–338, doi:10.1016/j.jhydrol.2018.10.022, 2018b.

710 Hao, Z., Hao, F., Singh, V. P. and Zhang, X.: Statistical prediction of the severity of  
711 compound dry-hot events based on El Niño–Southern Oscillation, J. Hydrol., 572,  
712 243–250, doi:10.1016/j.jhydrol.2019.03.001, 2019.

713 Hunt, E. D., Hubbard, K. G., Wilhite, D. A., Arkebauer, T. J. and Dutcher, A. L.: The  
714 development and evaluation of a soil moisture index. Int. J. Climatol., 29(5), 747-  
715 759, doi.org/10.1002/joc.1749, 2009.

716 James, S., Complex, B., Black, S. J., Health, O. and Ando, H.: The synergy between  
717 drought and extremely hot summers in the Mediterranean, Biochem. J., 2010.

718 Jiang, D., Tian, Z. and Lang, X.: Reliability of climate models for China through the  
719 IPCC Third to Fifth Assessment Reports, Int. J. Climatol., doi:10.1002/joc.4406,  
720 2016.

721 Kirono, D. G. C., Hennessy, K. J. and Grose, M. R.: Increasing risk of months with low  
722 rainfall and high temperature in southeast Australia for the past 150 years, Clim.



723 Risk Manag., doi:10.1016/j.crm.2017.04.001, 2017.

724 Koster, R. D., Schubert, S. D., Wang, H., Mahanama, S. P. and Deangelis, A. M.: Flash  
725 drought as captured by reanalysis data: Disentangling the contributions of  
726 precipitation deficit and excess evapotranspiration, *J. Hydrometeorol.*,  
727 doi:10.1175/JHM-D-18-0242.1, 2019.

728 [Liang, X., Wood, E. F., and Lettenmaier, D. P.: Surface soil moisture parameterization](#)  
729 [of the VIC-2L model: Evaluation and modification. \*Global and Planetary Change\*,](#)  
730 [13\(1-4\), 195-206, 1996.](#)

731 Li, J., Wang, Z., Wu, X., Chen, J., Guo, S., and Zhang, Z.: A new framework for  
732 tracking flash drought events in space and time. *Catena*, 194, 104763, 2020a.

733 Li, J., Wang, Z., Wu, X., Xu, C.-Y., Guo, S. and Chen, X.: Toward Monitoring Short-  
734 Term Droughts Using a Novel Daily-Scale, Standardized Antecedent Precipitation  
735 Evapotranspiration Index, *J. Hydrometeorol.*, 891–908, doi:10.1175/jhm-d-19-  
736 0298.1, 2020b.

737 Li, J., Wang, Z., Wu, X., Guo, S., and Chen, X.: Flash droughts in the Pearl River Basin,  
738 China: Observed characteristics and future changes. *Sci. Total Environ.*, 707,  
739 136074, 2020c.

740 Lin, W., Wen, C., Wen, Z. and Gang, H.: Drought in Southwest China: A Review,  
741 *Atmos. Ocean. Sci. Lett.*, 8(6), 339–344, doi:10.3878/AOSL20150043, 2015.

742 [Liu, Z., Wang, Y., Shao, M., Jia, X., Li, X: Spatiotemporal analysis of multiscalar](#)  
743 [drought characteristics across the Loess Plateau of China. \*J. Hydrol.\*, 534, 281-](#)  
744 [299, doi.org/10.1016/j.jhydrol.2016.01.003, 2016,](#)

745 Liu, Y., Zhu, Y., Ren, L., Singh, V. P., Yang, X. and Yuan, F.: A multiscalar Palmer  
746 drought severity index, *Geophys. Res. Lett.*, 44(13), 6850–6858,  
747 doi:10.1002/2017GL073871, 2017.

748 Liu, Y., Zhu, Y., Ren, L., Yong, B., Singh, V. P., Yuan, F., Jiang, S. and Yang, X.: On  
749 the mechanisms of two composite methods for construction of multivariate  
750 drought indices, *Sci. Total Environ.*, 647, 981–991,  
751 doi:10.1016/j.scitotenv.2018.07.273, 2019.

752 Liu, Y., Zhu, Y., Zhang, L., Ren, L., Yuan, F., Yang, X. and Jiang, S.: Flash droughts  
753 characterization over China: From a perspective of the rapid intensification rate,  
754 *Sci. Total Environ.*, doi:10.1016/j.scitotenv.2019.135373, 2020.

755 Lu, E.: Determining the start, duration, and strength of flood and drought with daily  
756 precipitation: Rationale, *Geophys. Res. Lett.*, 36(12), 1–5,  
757 doi:10.1029/2009GL038817, 2009.

758 Lu, E., Cai, W., Jiang, Z., Zhang, Q., Zhang, C., Higgins, R. W. and Halpert, M. S.:  
759 The day-to-day monitoring of the 2011 severe drought in China, *Clim. Dyn.*, 43(1–  
760 2), 1–9, doi:10.1007/s00382-013-1987-2, 2014.

761 Mo, K. C. and Lettenmaier, D. P.: Heat wave flash droughts in decline, *Geophys. Res.*  
762 *Lett.*, doi:10.1002/2015GL064018, 2015.

763 Mo, K. C. and Lettenmaier, D. P.: Precipitation deficit flash droughts over the United  
764 States, *J. Hydrometeorol.*, doi:10.1175/JHM-D-15-0158.1, 2016.

765 Mazdiyasni, O. and AghaKouchak, A.: Substantial increase in concurrent droughts and  
766 heatwaves in the United States, *Proc. Natl. Acad. Sci. U. S. A.*, 112(37), 11484–  
767 11489, doi:10.1073/pnas.1422945112, 2015.

768 ~~Miralles, D. G., Gentile, P., Seneviratne, S. I. and Teuling, A. J.: Land-atmospheric~~  
769 ~~feedbacks during droughts and heatwaves: state of the science and current~~  
770 ~~challenges, *Ann. N. Y. Acad. Sci.*, 1436(1), 19–35, doi:10.1111/nyas.13912, 2019.~~

771 Manning, C., Widmann, M., Bevacqua, E., Van Loon, A. F., Maraun, D. and Vrac, M:  
772 Increased probability of compound long-duration dry and hot events in Europe

773 during summer (1950-2013). Environmental Research Letters, 14(9), 094006,  
774 2019.

775 [Osman, M., Zaitchik, B. F., Badr, H. S., Christian, J. I., Tadesse, T., Otkin, J. A. and](#)  
776 [Anderson, M. C.: Flash drought onset over the Contiguous United States:](#)  
777 [Sensitivity of inventories and trends to quantitative definitions, Hydrol. Earth Syst.](#)  
778 [Sci. Discuss., doi.org/10.5194/hess-2020-385, in review, 2020.](#)

779 Otkin, J. A., Anderson, M. C., Hain, C., Mladenova, I. E., Basara, J. B. and Svoboda,  
780 M.: Examining rapid onset drought development using the thermal infrared-based  
781 evaporative stress index, J. Hydrometeorol., doi:10.1175/JHM-D-12-0144.1, 2013.

782 Otkin, J. A., Svoboda, M., Hunt, E. D., Ford, T. W., Anderson, M. C., Hain, C. and  
783 Basara, J. B.: Flash droughts: A review and assessment of the challenges imposed  
784 by rapid-onset droughts in the United States, Bull. Am. Meteorol. Soc., 99(5),  
785 911–919, doi:10.1175/BAMS-D-17-0149.1, 2018.

786 ~~Otkin, J. A., Zhong, Y., Hunt, E. D., Basara, J., Svoboda, M., Anderson, M. C. and~~  
787 ~~Hain, C.: Assessing the evolution of soil moisture and vegetation conditions~~  
788 ~~during a flash drought flash recovery sequence over the South Central United~~  
789 ~~States, J. Hydrometeorol., doi:10.1175/JHM-D-18-0171.1, 2019.~~

790 Pfliegerer, P., Schleussner, C. F., Kornhuber, K. and Coumou, D.: Summer weather  
791 becomes more persistent in a 2 °C world, Nat. Clim. Chang., 9(9), 666–671,  
792 doi:10.1038/s41558-019-0555-0, 2019.

793 Rodell, M., Houser, P. R., Jambor, U., Gottschalck, J., Mitchell, K., Meng, C. J.,  
794 Arsenault, K., Cosgrove, B., Radakovich, J., Bosilovich, M., Entin, J. K., Walker,  
795 J. P., Lohmann, D. and Toll, D.: The Global Land Data Assimilation System, Bull.  
796 Am. Meteorol. Soc., doi:10.1175/BAMS-85-3-381, 2004.

797 Röthlisberger, M. and Martius, O.: Quantifying the Local Effect of Northern

798 Hemisphere Atmospheric Blocks on the Persistence of Summer Hot and Dry  
799 Spells, *Geophys. Res. Lett.*, doi:10.1029/2019GL083745, 2019.

800 Schumacher, D. L., Keune, J., van Heerwaarden, C. C., Vilà-Guerau de Arellano, J.,  
801 Teuling, A. J. and Miralles, D. G.: Amplification of mega-heatwaves through heat  
802 torrents fuelled by upwind drought, *Nat. Geosci.*, 12(9), 712–717,  
803 doi:10.1038/s41561-019-0431-6, 2019.

804 Sedlmeier, K., Feldmann, H. and Schädler, G.: Compound summer temperature and  
805 precipitation extremes over central Europe, *Theor. Appl. Climatol.*,  
806 doi:10.1007/s00704-017-2061-5, 2018.

807 Stagge, J. H., Tallaksen, L. M., Gudmundsson, L., Van Loon, A. F. and Stahl, K.:  
808 Candidate Distributions for Climatological Drought Indices (SPI and SPEI), *Int. J.*  
809 *Climatol.*, doi:10.1002/joc.4267, 2015.

810 Seneviratne, S. I., Corti, T., Davin, E. L., Hirschi, M., Jaeger, E. B., Lehner, I., .and  
811 Teuling, A. J.: Investigating soil moisture–climate interactions in a changing  
812 climate: A review. *Earth-Science Reviews*, 99(3-4), 125-161, 2010.

813 Sun, C. and Yang, S.: Persistent severe drought in southern China during winter-spring  
814 2011: Large-scale circulation patterns and possible impacting factors, *J. Geophys.*  
815 *Res. Atmos.*, doi:10.1029/2012JD017500, 2012.

816 Sun, C. X., Huang, G. H., Fan, Y., Zhou, X., Lu, C. and Wang, X. Q.: Drought  
817 Occurring With Hot Extremes: Changes Under Future Climate Change on Loess  
818 Plateau, China, *Earth’s Futur.*, 7(6), 587–604, doi:10.1029/2018EF001103, 2019.

819 Swain, D. L., Langenbrunner, B., Neelin, J. D. and Hall, A.: Increasing precipitation  
820 volatility in twenty-first-century California, *Nat. Clim. Chang.*, 8(5), 427–433,  
821 doi:10.1038/s41558-018-0140-y, 2018.

822 Taylor, K. E., Stouffer, R. J. and Meehl, G. A.: An overview of CMIP5 and the

823 experiment design, Bull. Am. Meteorol. Soc., doi:10.1175/BAMS-D-11-00094.1,  
824 2012.

825 Terzi, S., Torresan, S., Schneiderbauer, S., Critto, A., Zebisch, M. and Marcomini, A.:  
826 Multi-risk assessment in mountain regions: A review of modelling approaches for  
827 climate change adaptation, J. Environ. Manage., 232(September 2018), 759–771,  
828 doi:10.1016/j.jenvman.2018.11.100, 2019.

829 Vicente-Serrano, S. M., Beguería, S. and López-Moreno, J. I.: A multiscalar drought  
830 index sensitive to global warming: The standardized precipitation  
831 evapotranspiration index, J. Clim., 23(7), 1696–1718,  
832 doi:10.1175/2009JCLI2909.1, 2010.

833 Wang, L., Yuan, X., Xie, Z., Wu, P. and Li, Y.: Increasing flash droughts over China  
834 during the recent global warming hiatus, Sci. Rep., doi:10.1038/srep30571, 2016.

835 Wang, W., Wang, W. J., Li, J. S., Wu, H., Xu, C. and Liu, T.: The impact of sustained  
836 drought on vegetation ecosystem in southwest China based on remote sensing, in  
837 Procedia Environmental Sciences., 2010.

838 Werner, A. T. and Cannon, A. J.: Hydrologic extremes - An intercomparison of multiple  
839 gridded statistical downscaling methods, Hydrol. Earth Syst. Sci.,  
840 doi:10.5194/hess-20-1483-2016, 2016.

841 Winston, H.A., Ruthi, L.J.: Evaluation of RADAP II severe-storm-detection algorithms.  
842 Bull. Am. Meteorol. Soc., 67(2), 145-150, doi.org/10.1175/1520-  
843 0477(1986)067<0145:EORISS>2.0.CO;2 1986.

844 Wu, J., Chen, X., Yao, H., Liu, Z. and Zhang, D.: Hydrological Drought Instantaneous  
845 Propagation Speed Based on the Variable Motion Relationship of Speed-Time  
846 Process, Water Resour. Res., doi:10.1029/2018WR023120, 2018.

847 Wu, X., Hao, Z., Hao, F. and Zhang, X.: Variations of compound precipitation and

848 temperature extremes in China during 1961–2014, *Sci. Total Environ.*, 663, 731–  
849 737, doi:10.1016/j.scitotenv.2019.01.366, 2019.

850 Wu, X., Hao, Z., Zhang, X., Li, C. and Hao, F.: Evaluation of severity changes of  
851 compound dry and hot events in China based on a multivariate multi-index  
852 approach, *J. Hydrol.*, 583, 124580, doi:10.1016/j.jhydrol.2020.124580, 2020.

853 Xia, Y., Mocko, D. M., Wang, S., Pan, M., Kumar, S. V., and Peters-Lidard, C. D.:  
854 Comprehensive evaluation of the variable infiltration capacity (VIC) model in the  
855 North American Land Data Assimilation System. *Journal of Hydrometeorology*,  
856 19(11), 1853-1879, 2018.

857 Xu, C., McDowell, N. G., Fisher, R. A., Wei, L., Sevanto, S., Christoffersen, B. O.,  
858 Weng, E. and Middleton, R. S.: Increasing impacts of extreme droughts on  
859 vegetation productivity under climate change, *Nat. Clim. Chang.*, 9(12), 948–953,  
860 doi:10.1038/s41558-019-0630-6, 2019.

861 Xu, K., Yang, D., Yang, H., Li, Z., Qin, Y. and Shen, Y.: Spatio-temporal variation of  
862 drought in China during 1961-2012: A climatic perspective, *J. Hydrol.*,  
863 doi:10.1016/j.jhydrol.2014.09.047, 2015.

864 Yang, Y., Bai, L., Wang, B., Wu, J. and Fu, S.: Reliability of the global climate models  
865 during 1961–1999 in arid and semiarid regions of China, *Sci. Total Environ.*,  
866 doi:10.1016/j.scitotenv.2019.02.188, 2019.

867 Yeo, I. N. K. and Johnson, R. A.: A new family of power transformations to improve  
868 normality or symmetry, *Biometrika*, 87(4), 954–959,  
869 doi:10.1093/biomet/87.4.954, 2000.

870 Yu, H., Zhang, Q., Xu, C. Y., Du, J., Sun, P. and Hu, P.: Modified Palmer Drought  
871 Severity Index: Model improvement and application, *Environ. Int.*, 130(January),  
872 104951, doi:10.1016/j.envint.2019.104951, 2019.

- 873 ~~Vogel, M. M., Zscheischler, J. and Seneviratne, S. I.: Varying soil moisture-atmosphere~~  
874 ~~feedbacks explain divergent temperature extremes and precipitation projections in~~  
875 ~~central Europe, Earth Syst. Dyn., doi:10.5194/esd-9-1107-2018, 2018.~~
- 876 Yuan, X., Wang, L., Wu, P., Ji, P., Sheffield, J. and Zhang, M.: Anthropogenic shift  
877 towards higher risk of flash drought over China, Nat. Commun.,  
878 doi:10.1038/s41467-019-12692-7, 2019.
- 879 ~~Zhang, Q., Li, Q., Singh, V. P., Shi, P., Huang, Q. and Sun, P.: Nonparametric~~  
880 ~~Integrated Agrometeorological Drought Monitoring: Model Development and~~  
881 ~~Application, J. Geophys. Res. Atmos., 123(1), 73–88, doi:10.1002/2017JD027448,~~  
882 ~~2018.~~
- 883 Zhang, W. J., Lu, Q. F., Gao, Z. Q. and Peng, J.: Response of remotely sensed  
884 normalized difference water deviation index to the 2006 drought of eastern  
885 Sichuan Basin, Sci. China, Ser. D Earth Sci., 51(5), 748–758, doi:10.1007/s11430-  
886 008-0037-0, 2008.
- 887 Zhang, Y., You, Q., Chen, C. and Li, X.: Flash droughts in a typical humid and  
888 subtropical basin: A case study in the Gan River Basin, China, J. Hydrol., 551,  
889 162–176, doi:10.1016/j.jhydrol.2017.05.044, 2017.
- 890 Zhang, Y., You, Q., Mao, G., Chen, C. and Ye, Z.: Short-term concurrent drought and  
891 heatwave frequency with 1.5 and 2.0 °C global warming in humid subtropical  
892 basins: a case study in the Gan River Basin, China, Clim. Dyn., 52(7–8), 4621–  
893 4641, doi:10.1007/s00382-018-4398-6, 2019.
- 894 Zhong, R., Chen, X., Lai, C., Wang, Z., Lian, Y., Yu, H. and Wu, X.: Drought  
895 monitoring utility of satellite-based precipitation products across mainland China,  
896 J. Hydrol., 568(June 2018), 343–359, doi: 10.1016/j.jhydrol.2018.10.072, 2019a.
- 897 Zhong, R., Zhao, T., He, Y. and Chen, X.: Hydropower change of the water tower of

898 Asia in 21st century: A case of the Lancang River hydropower base, upper  
899 Mekong, *Energy*, 179, 685–696, doi:10.1016/j.energy.2019.05.059, 2019b.

900 Zscheischler, J., Michalak, A. M., Schwalm, C., Mahecha, M. D. and Zeng, N.: Impact  
901 of large-scale climate extremes on biospheric carbon fluxes: An intercomparison  
902 based on MsTMIP data, *Global Biogeochem. Cycles*, 28(6), 585–600,  
903 doi:10.1002/2014GB004826, 2014.

904 Zscheischler, J., Orth, R. and Seneviratne, S. I.: Bivariate return periods of temperature  
905 and precipitation explain a large fraction of European crop yields, *Biogeosciences*,  
906 doi:10.5194/bg-14-3309-2017, 2017a.

907 Zscheischler, J. and Seneviratne, S. I.: Dependence of drivers affects risks associated  
908 with compound events, *Sci. Adv.*, 3(6), 1–11, doi:10.1126/sciadv.1700263, 2017b.

909 Zscheischler, J., Westra, S., Van Den Hurk, B. J. J. M., Seneviratne, S. I., Ward, P. J.,  
910 Pitman, A., Aghakouchak, A., Bresch, D. N., Leonard, M., Wahl, T. and Zhang,  
911 X.: Future climate risk from compound events, *Nat. Clim. Chang.*, 8(6), 469–477,  
912 doi:10.1038/s41558-018-0156-3, 2018.

913 Zscheischler, J., Martius, O., Westra, S., Bevacqua, E. and Raymond, C.: A typology  
914 of compound weather and climate events, *Nat. Rev. Earth Environ.*, doi:  
915 <https://doi.org/10.1038/s43017-020-0060-z>, 2020.

916 Zhou, J., Wu, Z., He, H., Wang, F., Xu, Z., and Wu, X.: Regional assimilation of in situ  
917 observed soil moisture into the VIC model considering spatial variability.  
918 Hydrological Sciences Journal, 64(16), 1982-1996, 2019

919

920

921

922

923



924 **Table**

925 Table 1 Categories of compound dry and hot conditions based on SCDHI.

Category	Dry and hot condition	SCDHI
<u>G</u> Grade 0 <sub>0</sub>	Abnormal	(-0.80, -0.50]
<u>Grade</u>	Light	(-1.30, -0.80]
<u>0G</u> <sub>1</sub>		
<u>Grade</u>	Moderate	(-1.60, -1.30]
<u>0G</u> <sub>2</sub>		
<u>Grade</u>	Heavy	(-2.0, -1.60]
<u>0G</u> <sub>3</sub>		
<u>Grade</u>	Extreme	≤ -2
<u>0G</u> <sub>4</sub>		

926

927

928

929

930

931

932

933

934

935

936

937

938

939

940

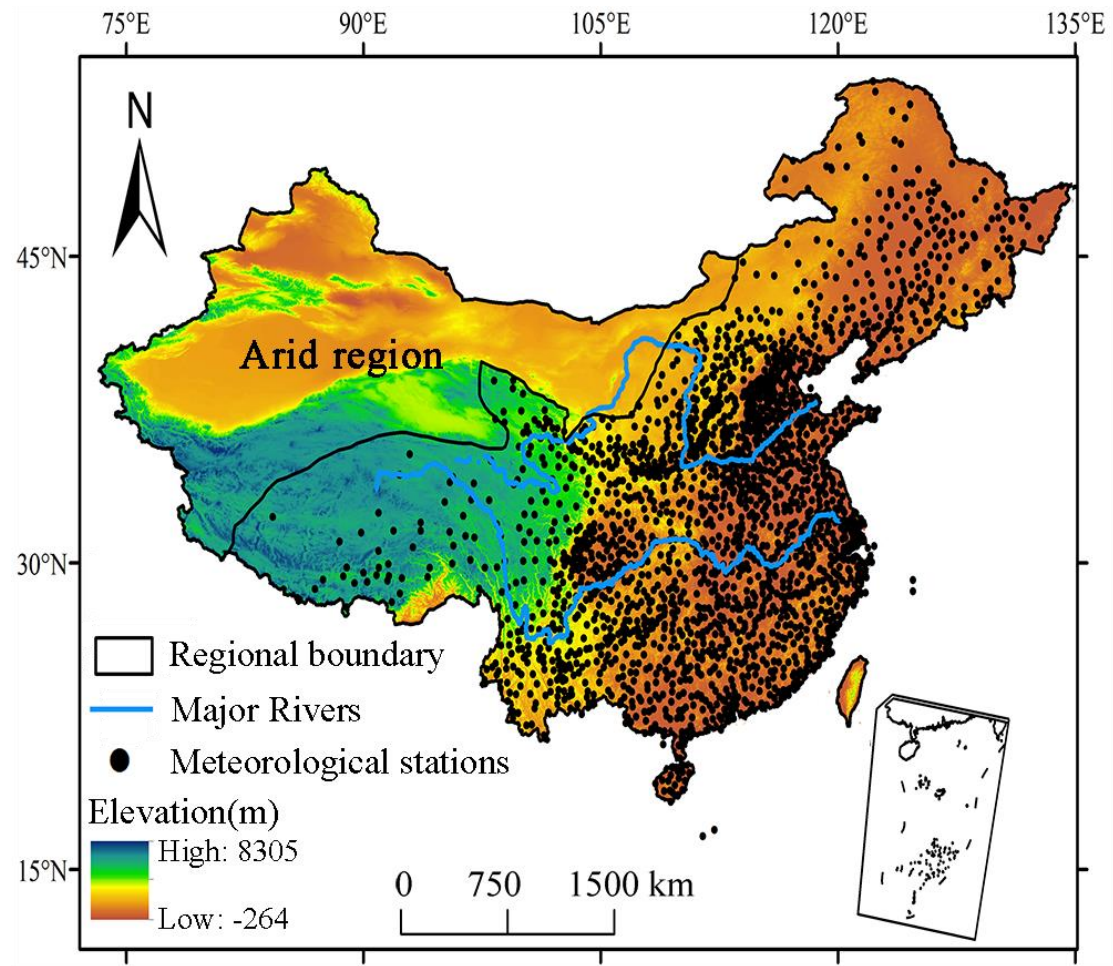
941

942

943

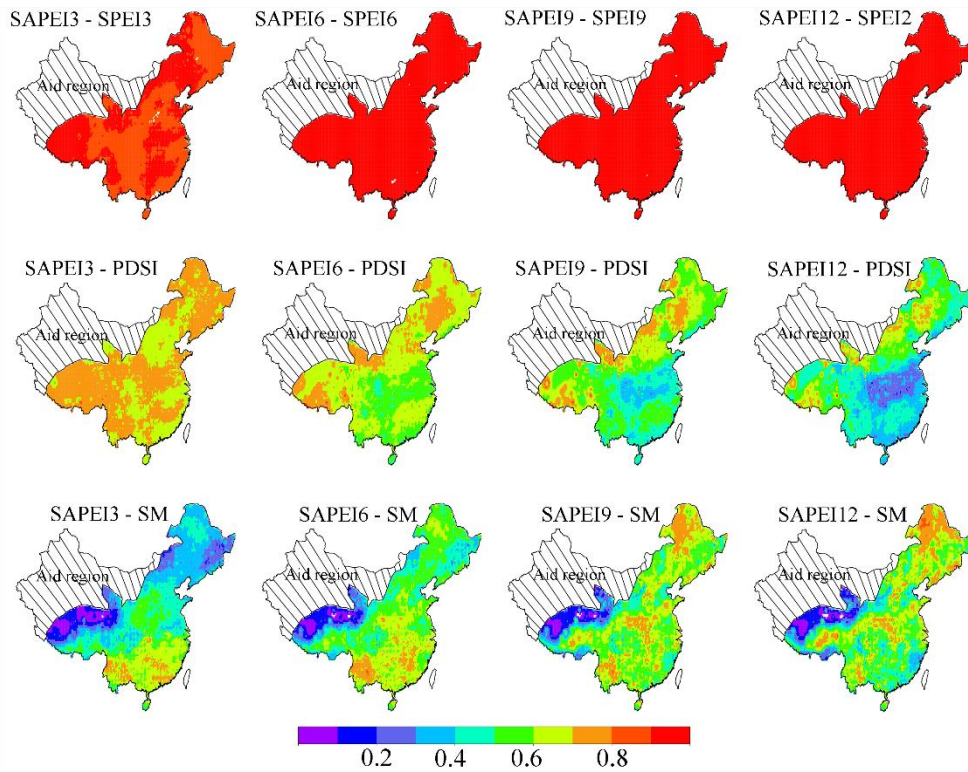
944  
945  
946

947 **Figure**

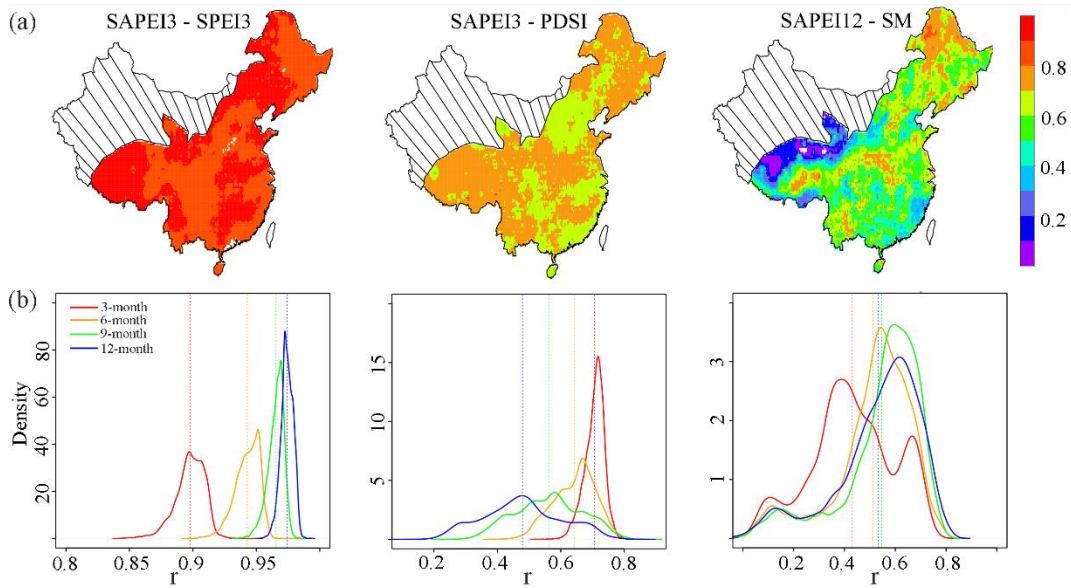


948  
949  
950  
951  
952  
953  
954  
955  
956  
957

Figure 1 Geographical position of China and local of meteorological stations.

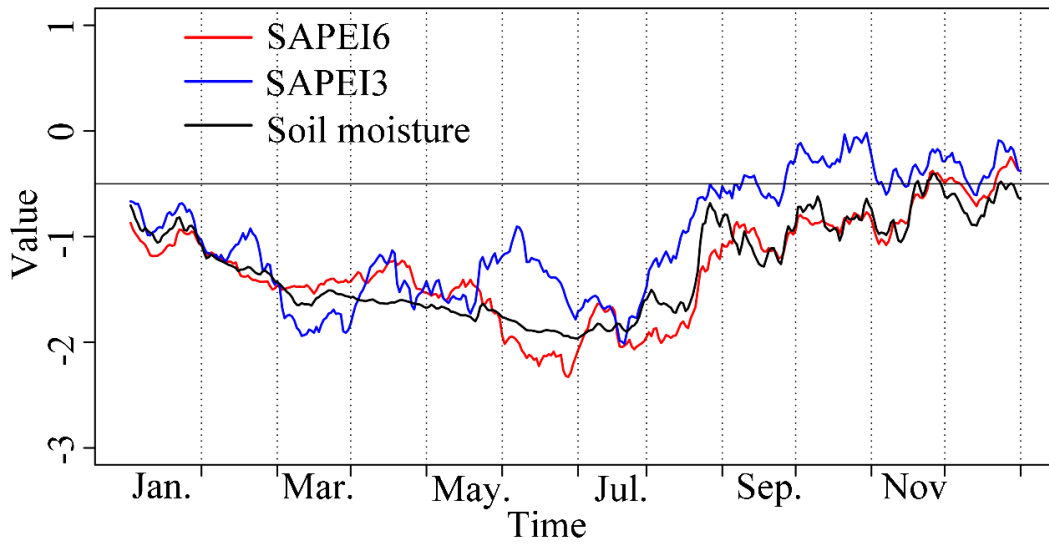


958



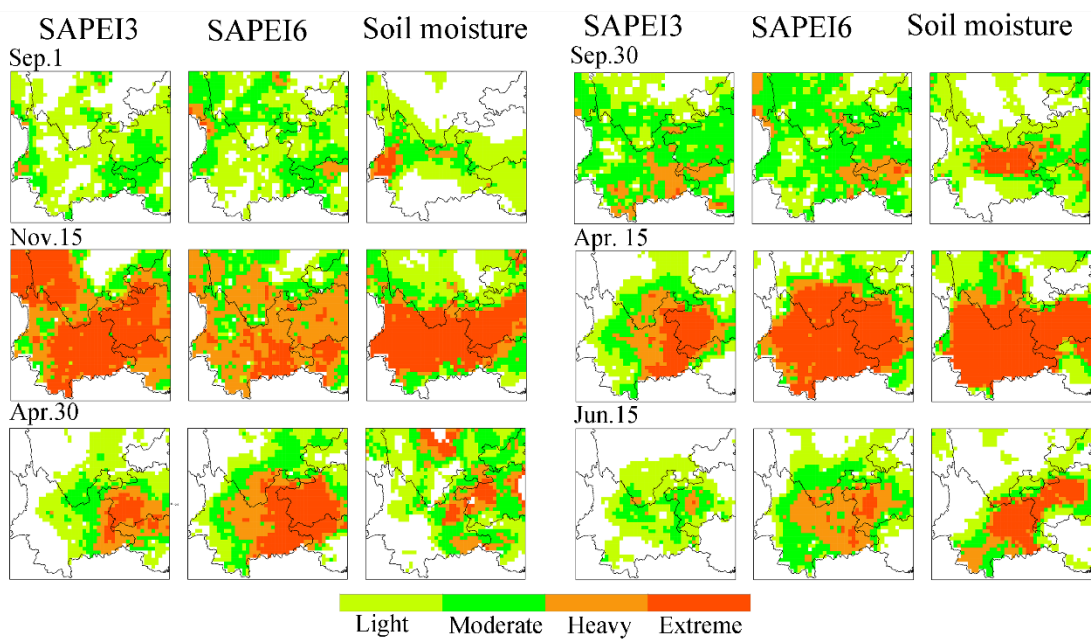
959

960 Figure 2 (a) The spatial pattern of the correlations between monthly SAPEI and  
 961 SPEI/PDSI, and between daily SAPEI and soil moisture (SM), and (b) The density plot  
 962 for the correlations. The monthly SAPEI is computed by averaging the daily values in  
 963 each month.

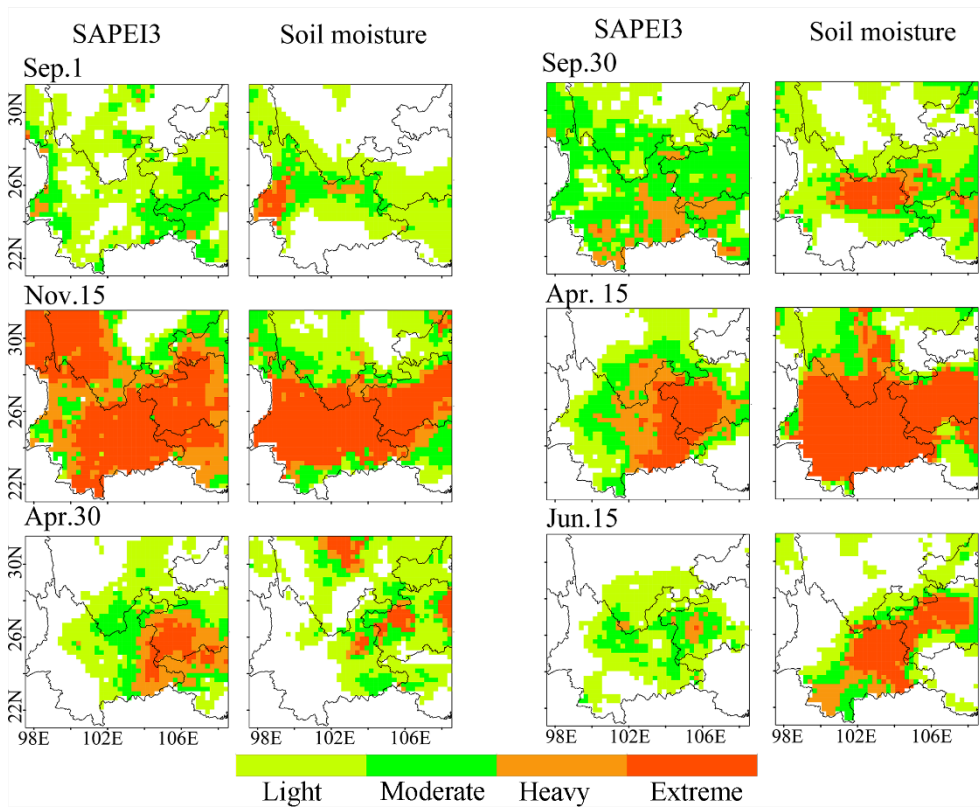


964

965 Figure 3 SAPEI (3 and 6 month) and soil moisture series during the 2009/2010 drought  
 966 event over the southwest China. The series were spatially average merged series. The  
 967 value of solid black line is at -0.5, indicating the distinction between drought and non-  
 968 drought.



969

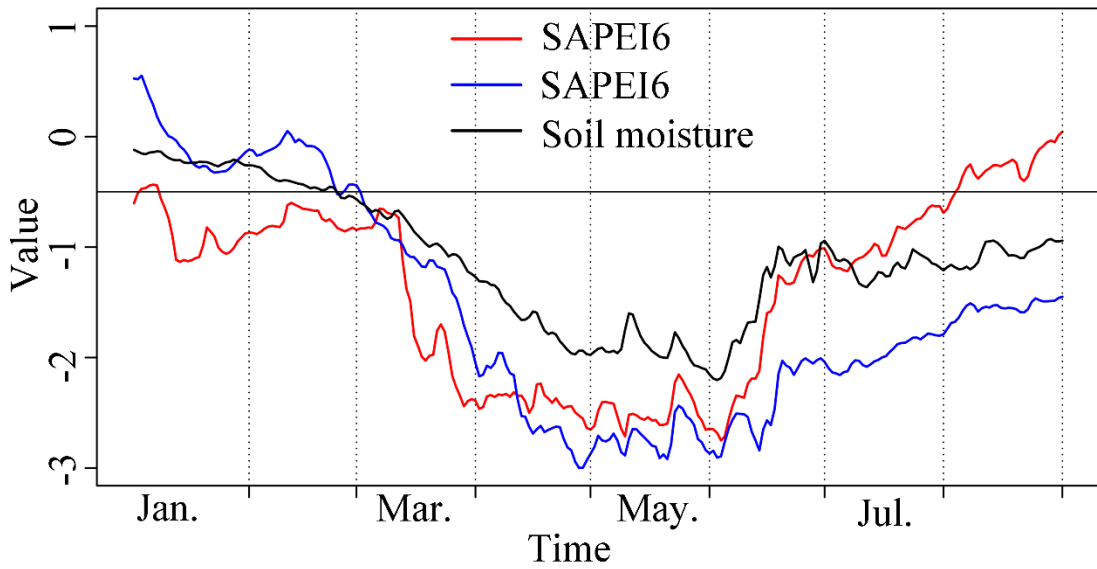


970

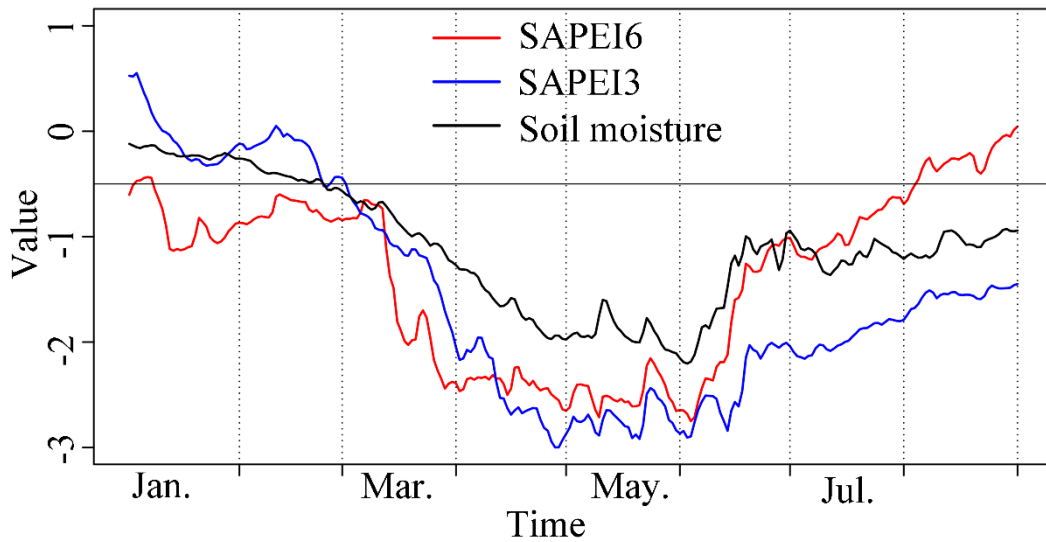
971 Figure 4 Daily evolutions of the 2009/2010 drought event over the southwest China

972 monitored by 3- and 6-month SAPEI and soil moisture.

973



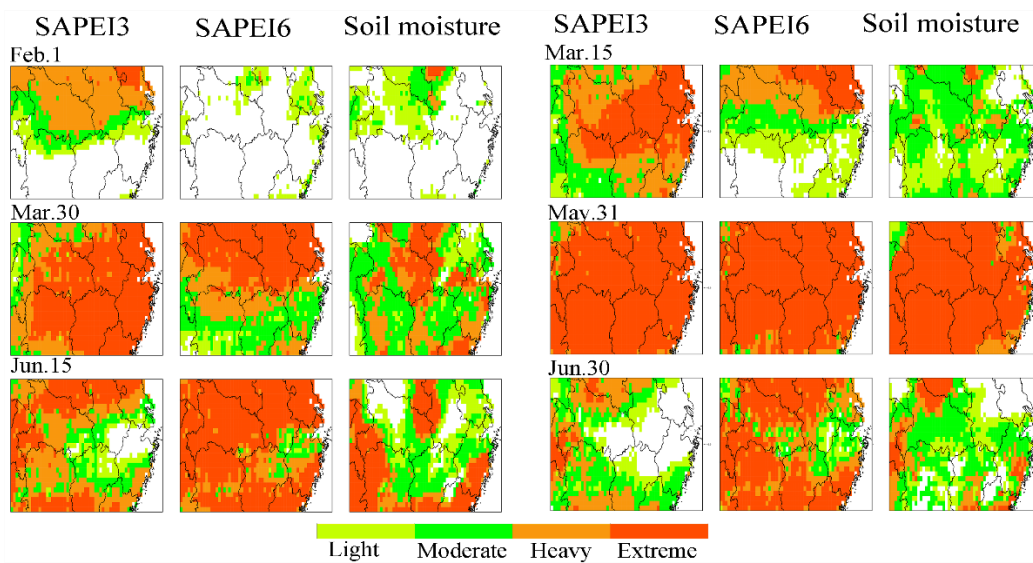
974



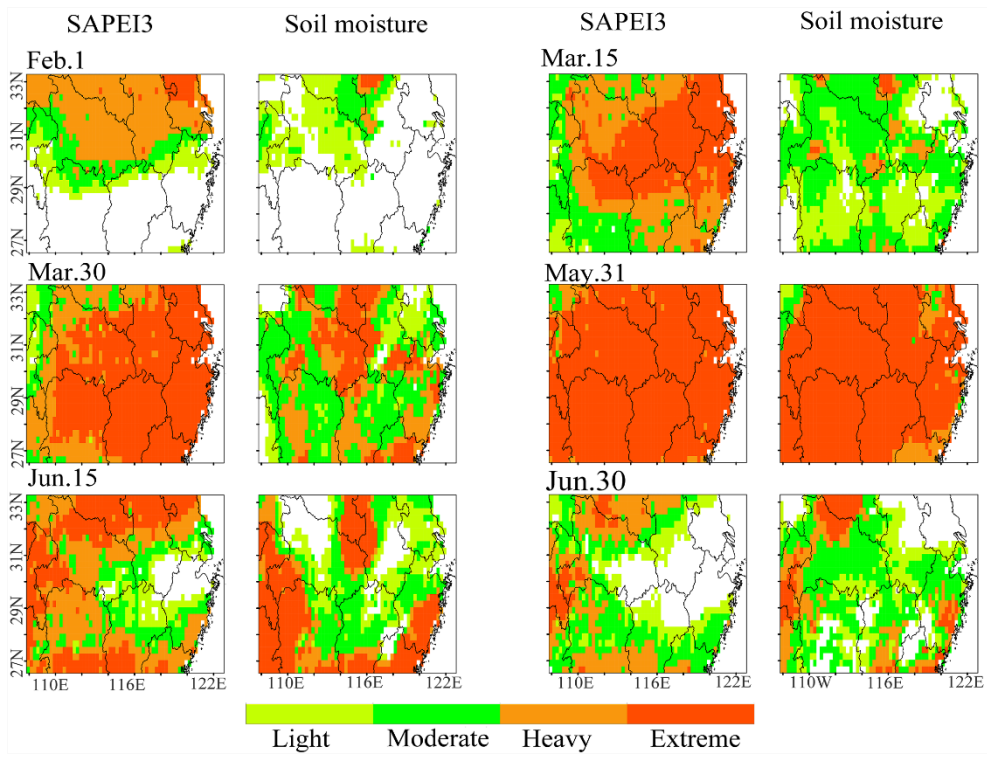
975

976 Figure 5 SAPEI (3- and 6-month) and soil moisture series during the 2011 drought  
 977 event over the middle and lower reaches of the Yangtze River. The series were spatially  
 978 average merged series. The value of solid black line is at -0.5, indicating the distinction  
 979 between drought and non-drought.

980



981



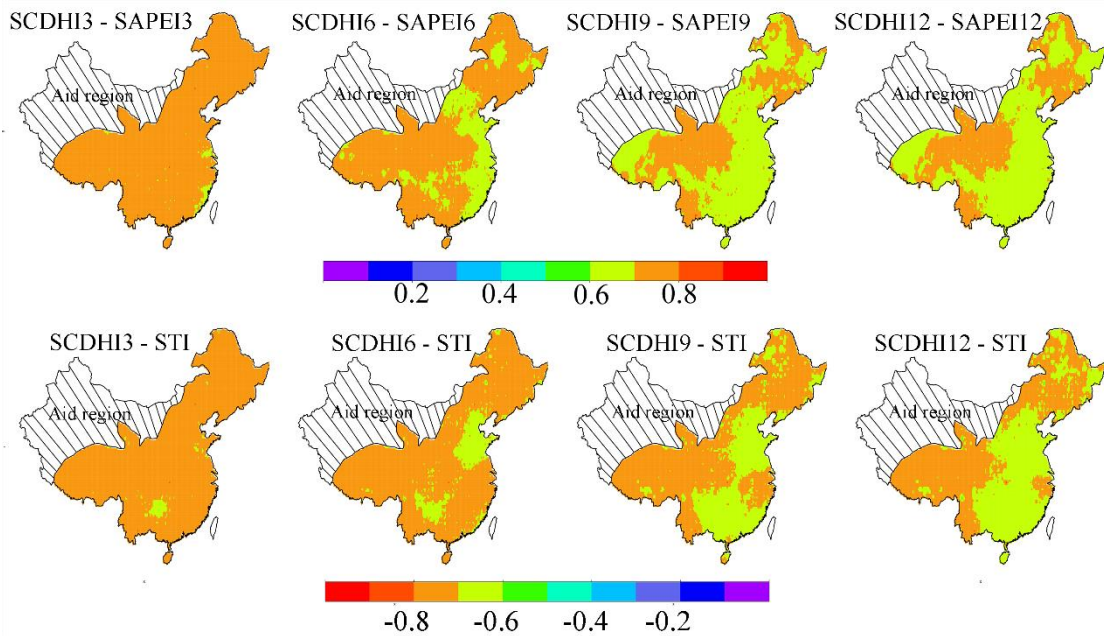
982

983 Figure 6 Daily evolutions of the 2011 drought event over the middle and lower reaches

984 of the Yangtze River monitored by 3-~~and 6~~-month SAPEI and soil moisture.

985

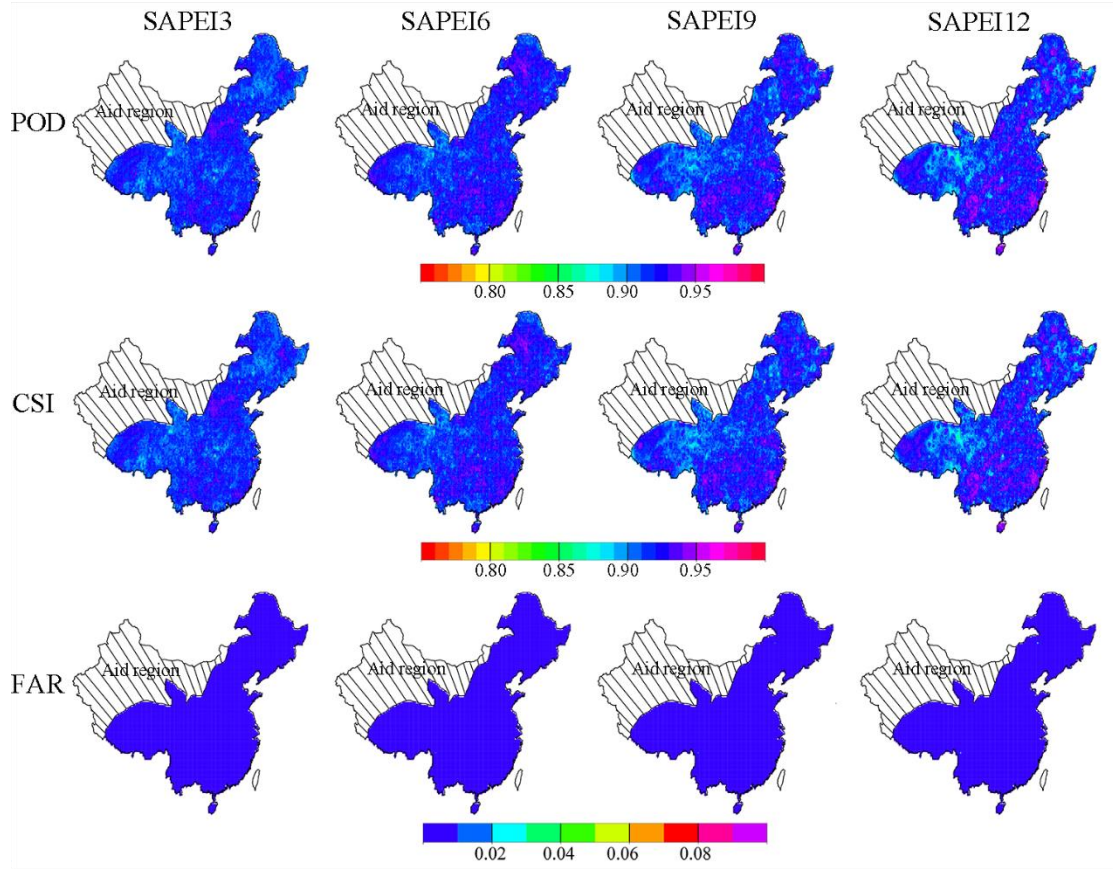
986



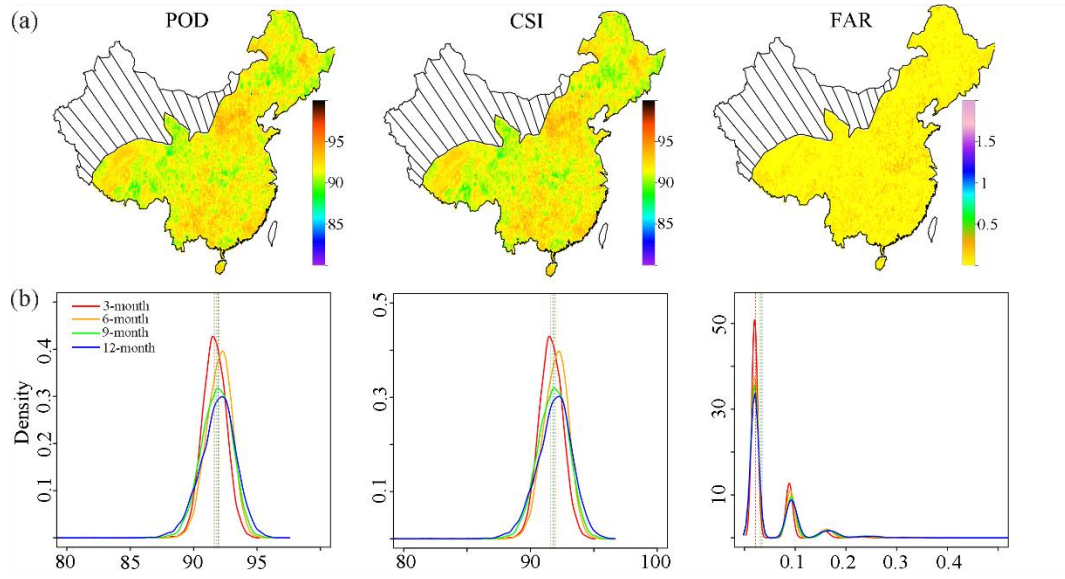
987

988 Figure 7 The spatial pattern of the correlations between SCDHI and SAPEI/STI at daily

989 scale from 1961 to 2018.



990

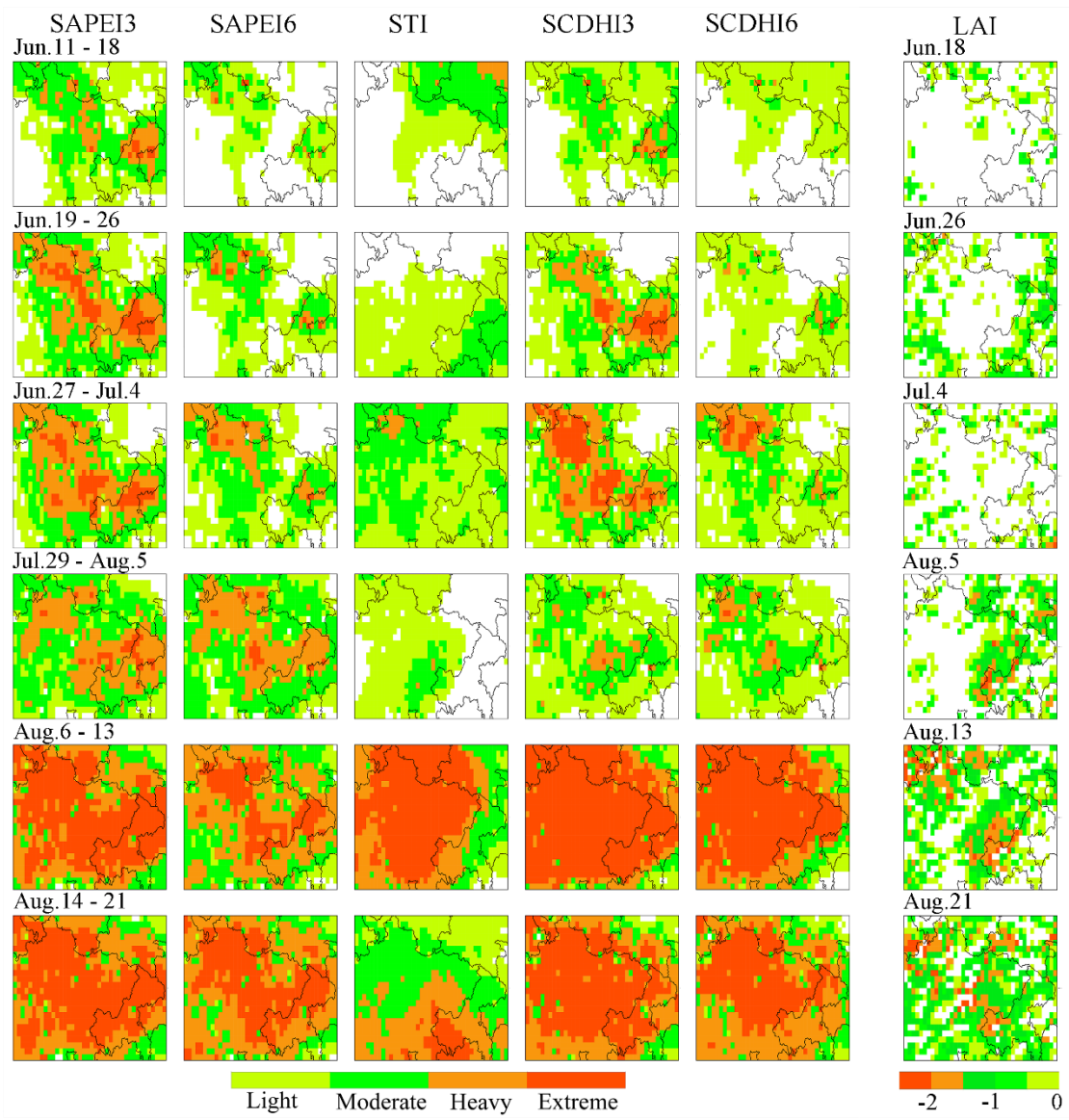


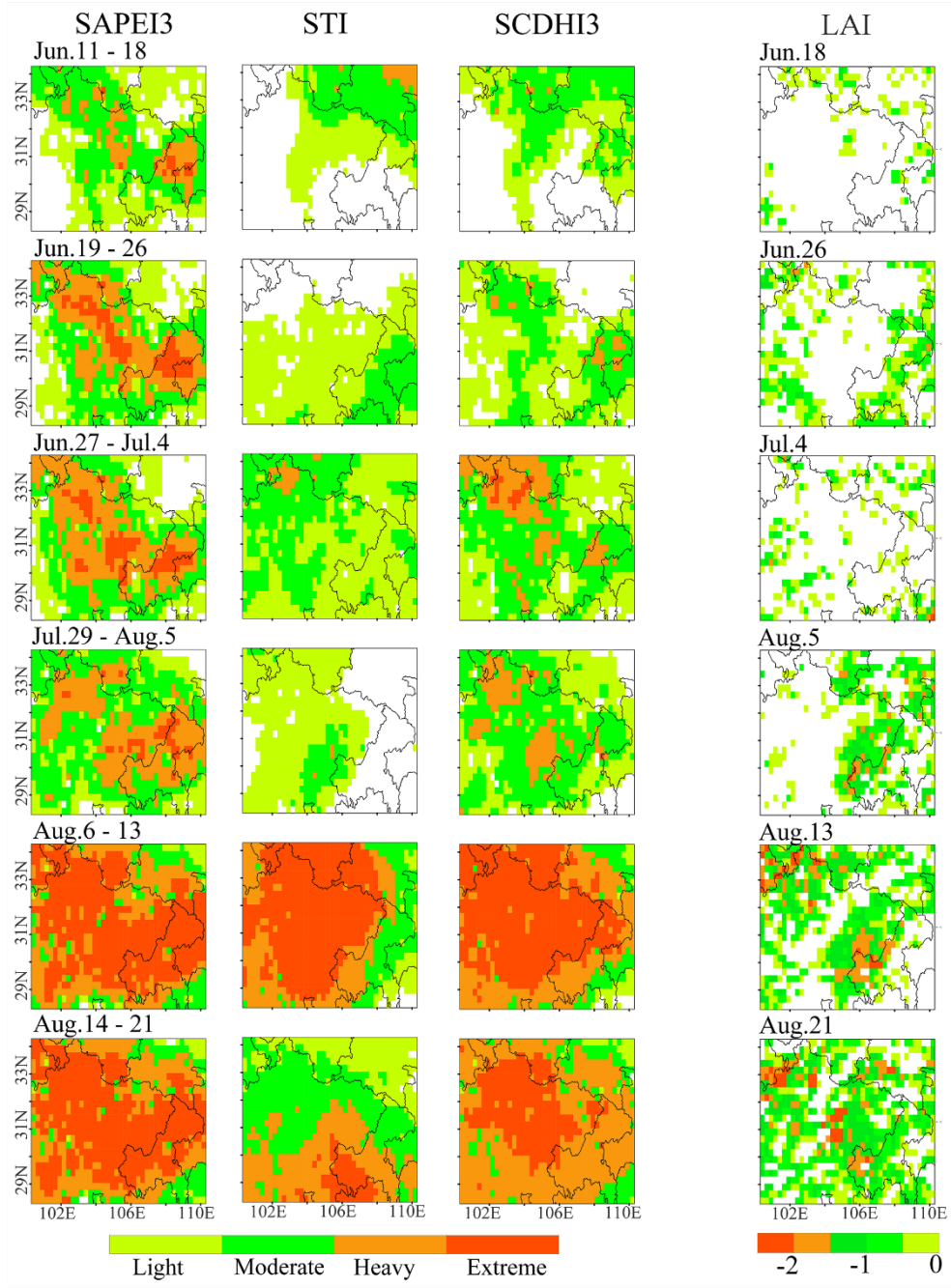
991

992 Figure 8-7 (a) The spatial pattern of probability of detection (POD)POD (%), FAR, and  
 993 critical success index (CSI)CSI (%), and false alarm ratio (FAR) for 3-month SCDHI  
 994 at 3-, 6-, 9- and 12-month time scales from 1961 to 2018, and (b) Density plot for POD,  
 995 FAR, and CSI for 3-, 6-, 9-, 12-month SCDHI from 1961 to 2018.

996







998

999 Figure 98: The spatial evolutions of the compound dry and hot event over the Sichuan-

1000

Chongqing region in 2006 and its impact on vegetation.

1001

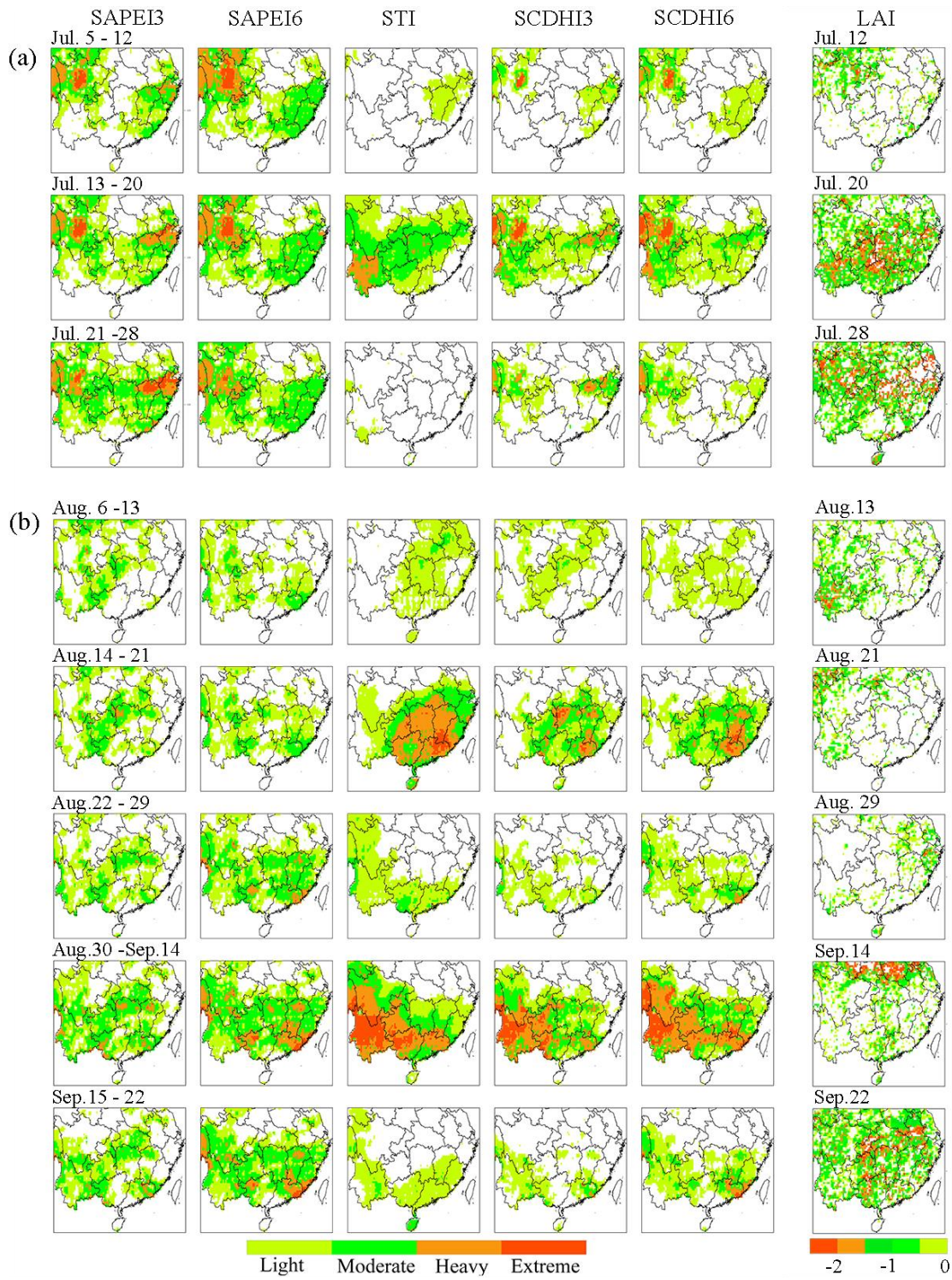
1002

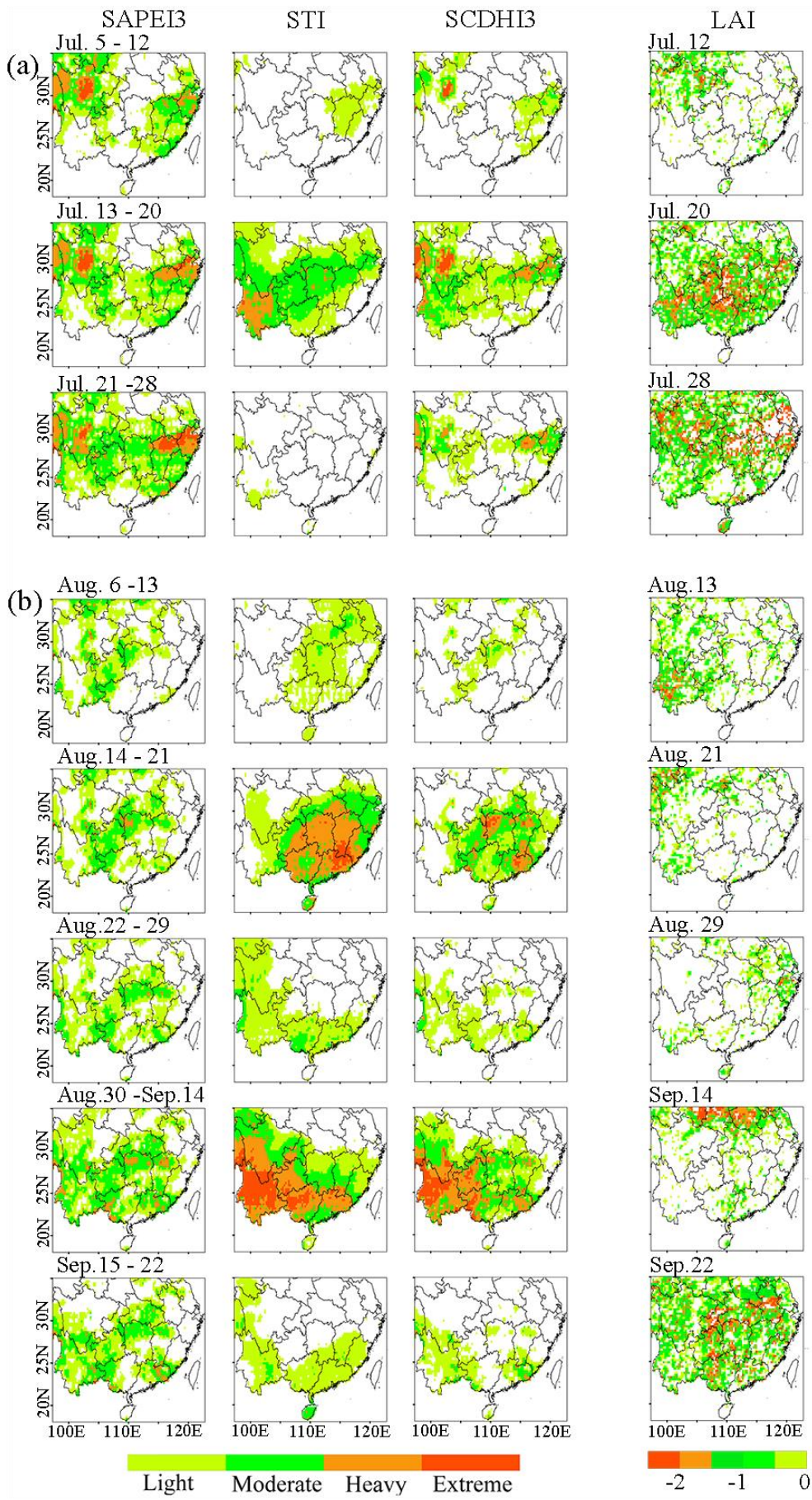
1003

1004

1005

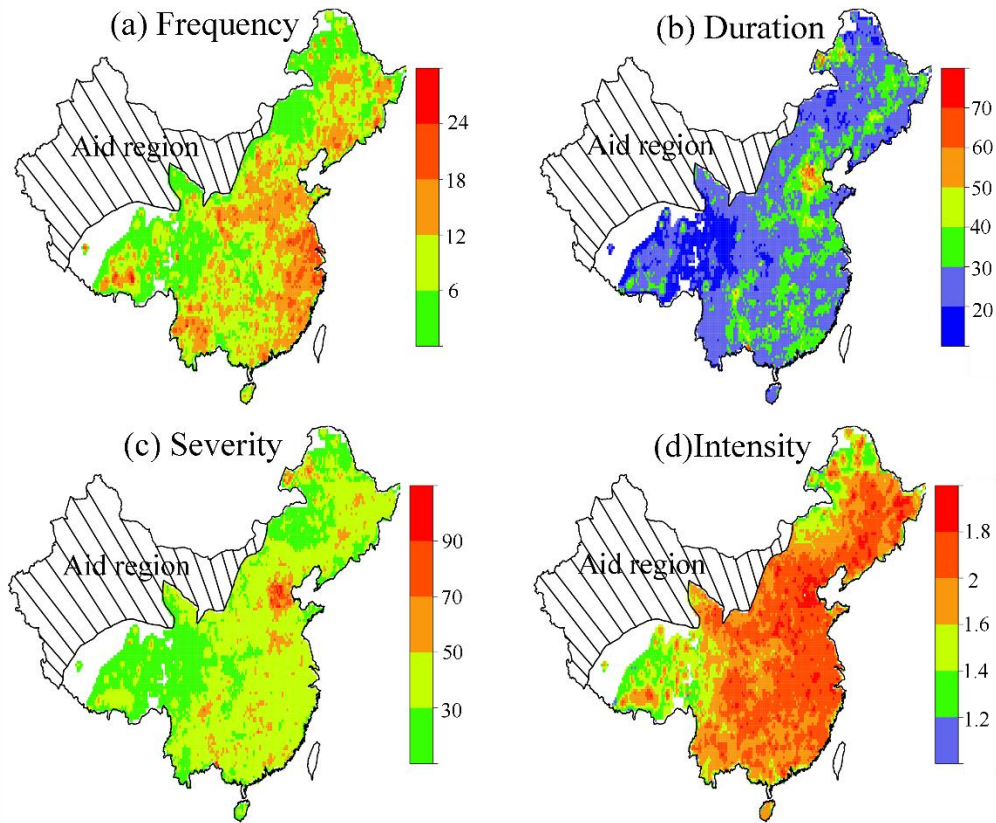
1006



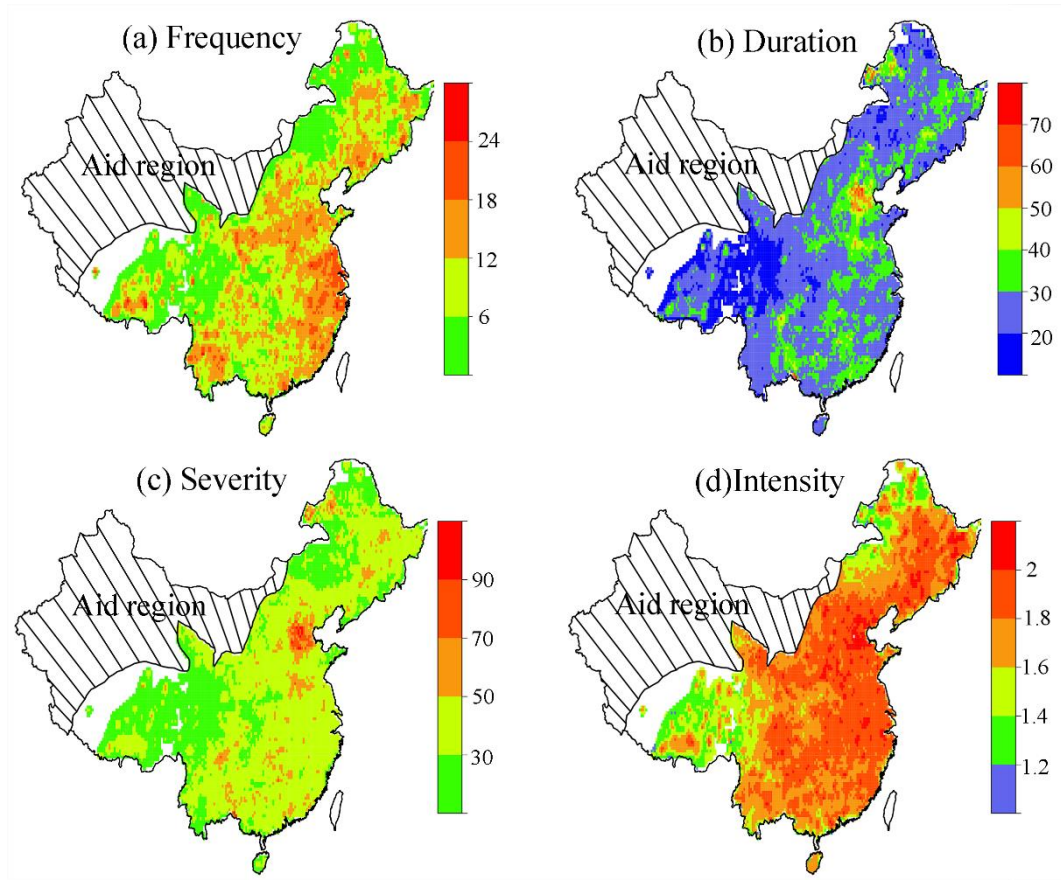


1009 Figure 10-9 The spatial evolutions of the compound dry and hot event over the southern  
1010 China in 2009 and its impact on vegetation.

1011  
1012  
1013



1014



1015

1016 Figure 4-10 The spatial pattern of the characteristics of the compound dry and hot

1017 event in China from 1961 to 2018.

1018

1019

1020

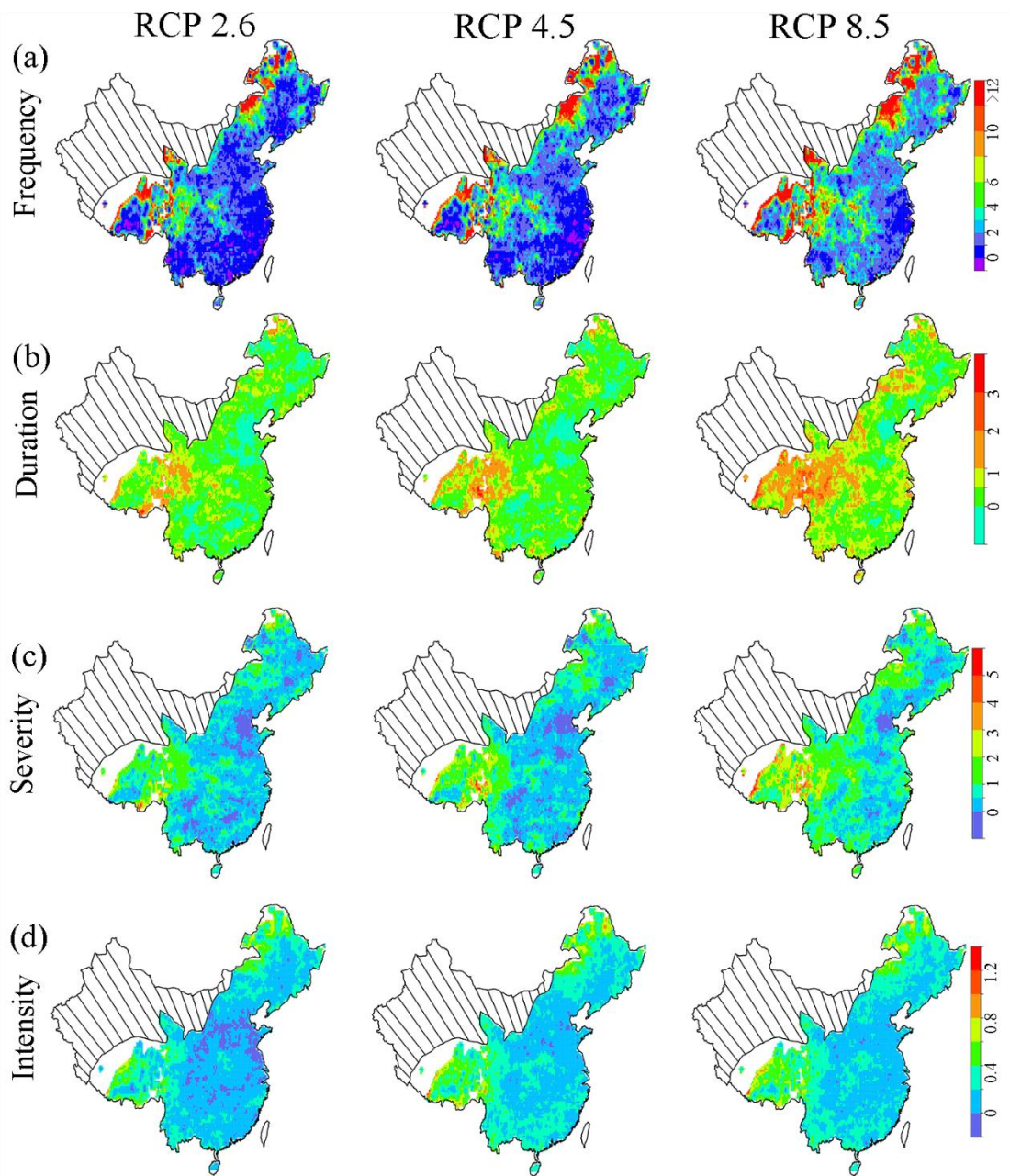
1021

1022

1023

1024

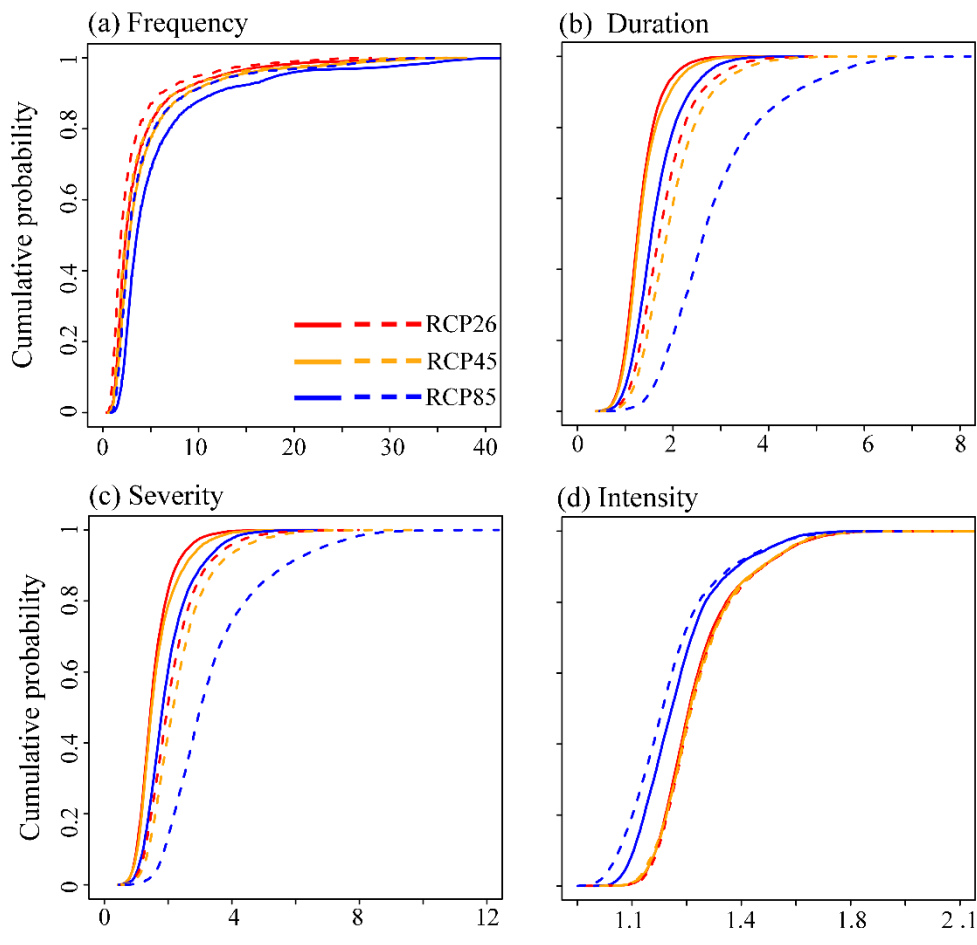
1025



1026

1027 Figure 12-11 Future changes in characteristics of the compound dry and hot events  
 1028 under the RCP 2.6, RCP4.5 and RCP8.5 scenarios. The change values were the ratio of  
 1029 the future value to the reference values. Reference period: 1961-2018, and future period:  
 1030 2050-2100.

1031



1032

1033

1034

1035

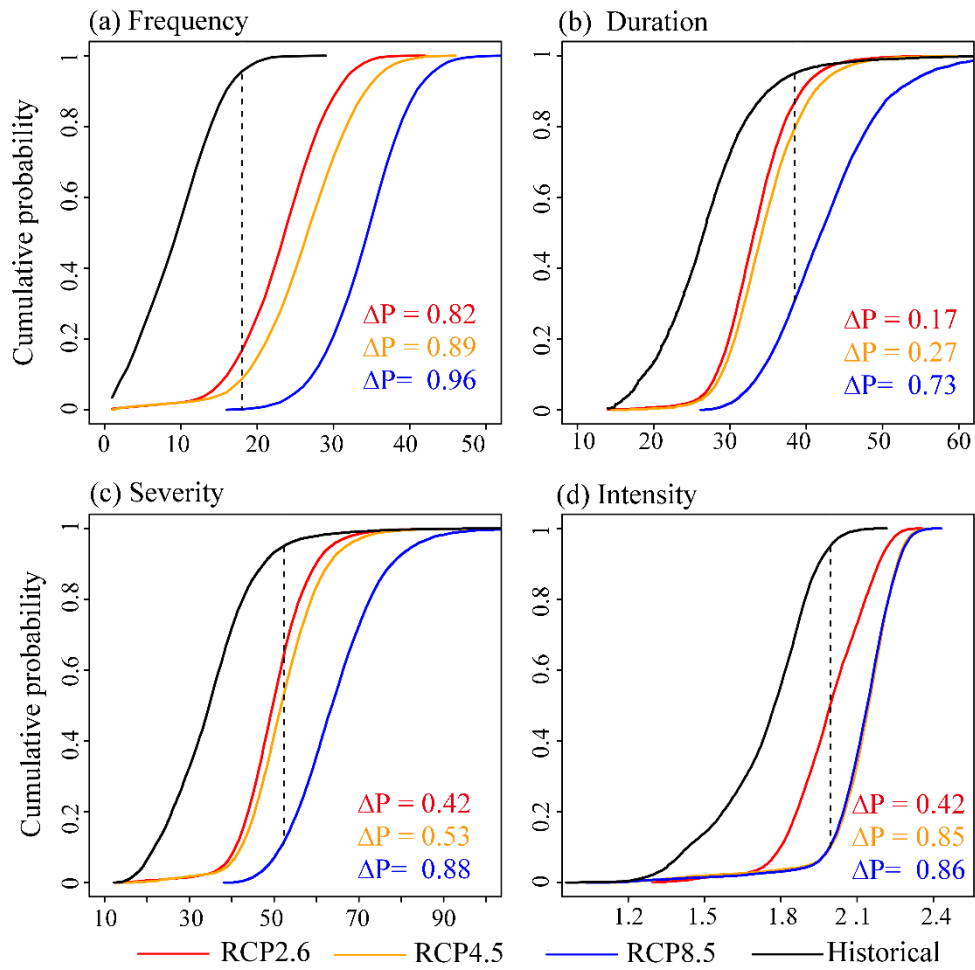
1036

1037

1038

Figure 12 Cumulative probability of future changes (multiple) in of the compound dry-hot event characteristics. The dash lines indicate future characteristics changes only considered temperature change, while solid lines represent the future changes driven by all variable variation.





1039

1040 Figure 13 Cumulative probability functions of characteristics of the compound drought

1041 and hot events in historical and future period. The vertical lines denote the probability

1042 of the 95<sup>th</sup> percentile value during the historical period.  $\Delta P$  denotes the changes in the

1043 probability of the 95<sup>th</sup> percentile value between the historical period and the future

1044 period. Reference period: 1961–2018, and future period: 2050–2100. The red, orange,

1045 and blue fonts refer to the change values under RCP 2.6, 4.5 and 8.5 scenario,

1046 respectively.

1047